Science of the Total Environment 940 (2024) 173440

Contents lists available at ScienceDirect

Science of the Total Environment

journal homepage: www.elsevier.com/locate/scitotenv

Terrestrial inputs boost organic carbon accumulation in Mexican mangroves

J.L.J. Jupin [a,b], A.C. Ruiz-Fernández [c,*], A. Sifeddine [b], M. Mendez-Millan [b], J.A. Sanchez-Cabeza [c], L.H. Pérez-Bernal [c], J.G. Cardoso-Mohedano [d], M.A. Gómez-Ponce [d], J.G. Flores-Trujillo [e]

[a] Posgrado en Ciencias del Mar y Limnología, Universidad Nacional Autónoma de México, Av. Universidad 3000, Ciudad Universitaria, Coyoacán, 04510 Ciudad de México, Mexico
[b] IRD, CNRS, SU, MNHN, IPSL, LOCEAN, Laboratoire d'Océanographie et du Climat: Expérimentation et Approches Numériques Centre IRD France Nord, 93143 Bondy, France
[c] Unidad Académica Mazatlán, Instituto de Ciencias del Mar y Limnología, Universidad Nacional Autónoma de México, 82040 Mazatlán, Sin., Mexico
[d] Estación el Carmen, Instituto de Ciencias del Mar y Limnología, Universidad Nacional Autónoma de México, Carretera Carmen-Puerto Real km 9.5, 24157 Ciudad del Carmen, Campeche, Mexico
[e] Universidad Autónoma del Carmen, Calle 56 No. 4, Col. Benito Juárez, 24180 Cd. del Carmen, Camp., Mexico

HIGHLIGHTS

- Burial rates and stocks of mangrove sediment organic carbon (C_{org}) are reported.
- Highest C_{org} stocks was observed in sites with autochthonous-dominated C_{org}.
- Global C_{org} patterns do not fully explain the local C_{org} variability in study sites.
- Long-term rise in terrestrial C_{org} inputs led to higher C_{org} burial rates and stocks.
- Despite cover loss, mangroves areas remained effective C_{org} producers and sinks.

GRAPHICAL ABSTRACT

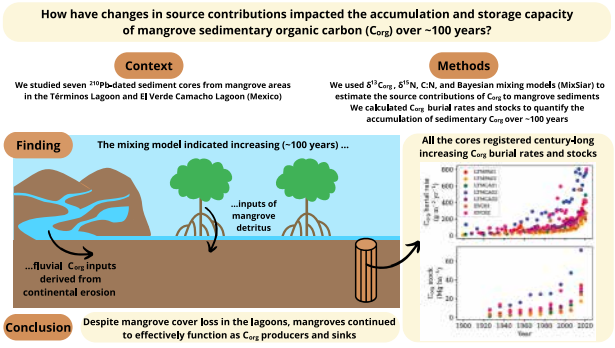

ARTICLE INFO

Editor: Jan Vymazal

Keywords:
Blue carbon
Burial rate
Stock
Mangroves

ABSTRACT

Despite their ability to mitigate climate change by efficiently absorbing atmospheric carbon dioxide (CO_2) and acting as natural long-term carbon sinks, mangrove ecosystems have faced several anthropogenic threats over the past century, resulting in a decline in the global mangrove cover. By using standardized methods and the most recent Bayesian tracer mixing models MixSIAR, this study aimed to quantify source contributions, burial rates, and stocks of organic carbon (C_{org}) and explore their temporal changes (~100 years) in seven lead-210 dated sediment cores collected from three contrasting Mexican mangrove areas. The spatial variation in C_{org} burial rates and stocks in these blue carbon ecosystems primarily depended on the influence of local rivers, which

* Corresponding author.
E-mail addresses: caro@ola.icmyl.unam.mx (A.C. Ruiz-Fernández), abdel.sifeddine@ird.fr (A. Sifeddine), mercedes.mendez@ird.fr (M. Mendez-Millan), jasanchez@cmarl.unam.mx (J.A. Sanchez-Cabeza), lbernal@ola.icmyl.unam.mx (L.H. Pérez-Bernal), gcardoso@cmarl.unam.mx (J.G. Cardoso-Mohedano), mgomez@cmarl.unam.mx (M.A. Gómez-Ponce), gflores@pampano.unacar.mx (J.G. Flores-Trujillo).

https://doi.org/10.1016/j.scitotenv.2024.173440
Received 26 February 2024; Received in revised form 29 April 2024; Accepted 20 May 2024
Available online 25 May 2024

^{210}Pb radiochronology
MixSIAR

controlled C_{org} sources and fluxes within the mangrove areas. The C_{org} burial rates in the cores ranged from 66 ± 16 to 400 ± 40 g m^{-2} yr^{-1}. The C_{org} stocks ranged from 84.9 ± 0.7 to 255 ± 2 Mg ha^{-1} at 50 cm depth and from 137 ± 2 to 241 ± 4 Mg ha^{-1} at 1 m depth. The highest C_{org} burial rates and stocks were observed in cores from the carbonate platform of Yucatan and in cores with reduced river influence and high mangrove detritus inputs, in contrast to patterns identified from global databases. Over the past century, the rising trends in C_{org} burial rates and stocks in the study sites were primarily driven by enhanced inputs of fluvial-derived C_{org} and, in some cores, mangrove-derived C_{org}. Despite their decreasing extension, mangrove areas remained highly effective producers and sinks of C_{org}. Ongoing efforts to enhance the global database should continue, including mangrove area characteristics and reliable timescales to facilitate cross-comparison among studies.

1. Introduction

Despite the multiple benefits provided by mangroves (Blankespoor et al., 2017; Primavera et al., 2019b), the world's mangrove cover has declined due to land-use changes, particularly the conversion of mangroves to aquaculture and agriculture areas (Goldberg et al., 2020; Valiela et al., 2001). Thanks to the implementation of conservation policies, the worldwide rate of mangrove cover loss is now lower than in the past (i.e., >2 % in 1980–2005, FAO, 2007; 0.16–0.39 % in 2000–2012, Hamilton and Casey, 2016). Nevertheless, the loss rates vary among countries (e.g., 0.7 % in Myanmar, 0.08 % in Mexico, and 0.03 % in Australia between 2000 and 2012; Hamilton and Casey, 2016) due to differences in mangrove management policies and regulations, economic conditions, and demography (Primavera et al., 2019a). In addition, the loss rates do not provide information about the conservation status of the remaining forests nor the magnitude of potential loss in ecosystem services and carbon storage.

The extent of ecosystem service loss resulting from mangrove cover loss varies depending on the type of mangrove and the hydrologic and biogeographic characteristics of the region. Furthermore, a large fraction of sedimentary organic carbon (C_{org}) stocks in degraded mangrove ecosystems may be oxidized to carbon dioxide (CO_2) and released into the atmosphere, contributing to global warming (Hamilton and Friess, 2018; Kauffman et al., 2014). Therefore, the conservation and restoration of mangroves are significant and low-cost strategies for climate change mitigation to reduce atmospheric CO_2 (Murdiyarso et al., 2015; Pendleton et al., 2012), needed to keep global warming under 2 °C by 2050 (UN, 2015).

The study of C_{org} burial rates and stocks is essential for conducting comprehensive assessments of actual and past C_{org} storage in mangroves. The wide ranges of C_{org} stocks (72–936 Mg ha^{-1}; Atwood et al., 2017) and C_{org} burial rates (2.3–1750 g m^{-2} yr^{-1}; Breithaupt and Steinmuller, 2022) in mangrove ecosystems worldwide result from the strong spatial and temporal heterogeneity of processes (e.g., climate,

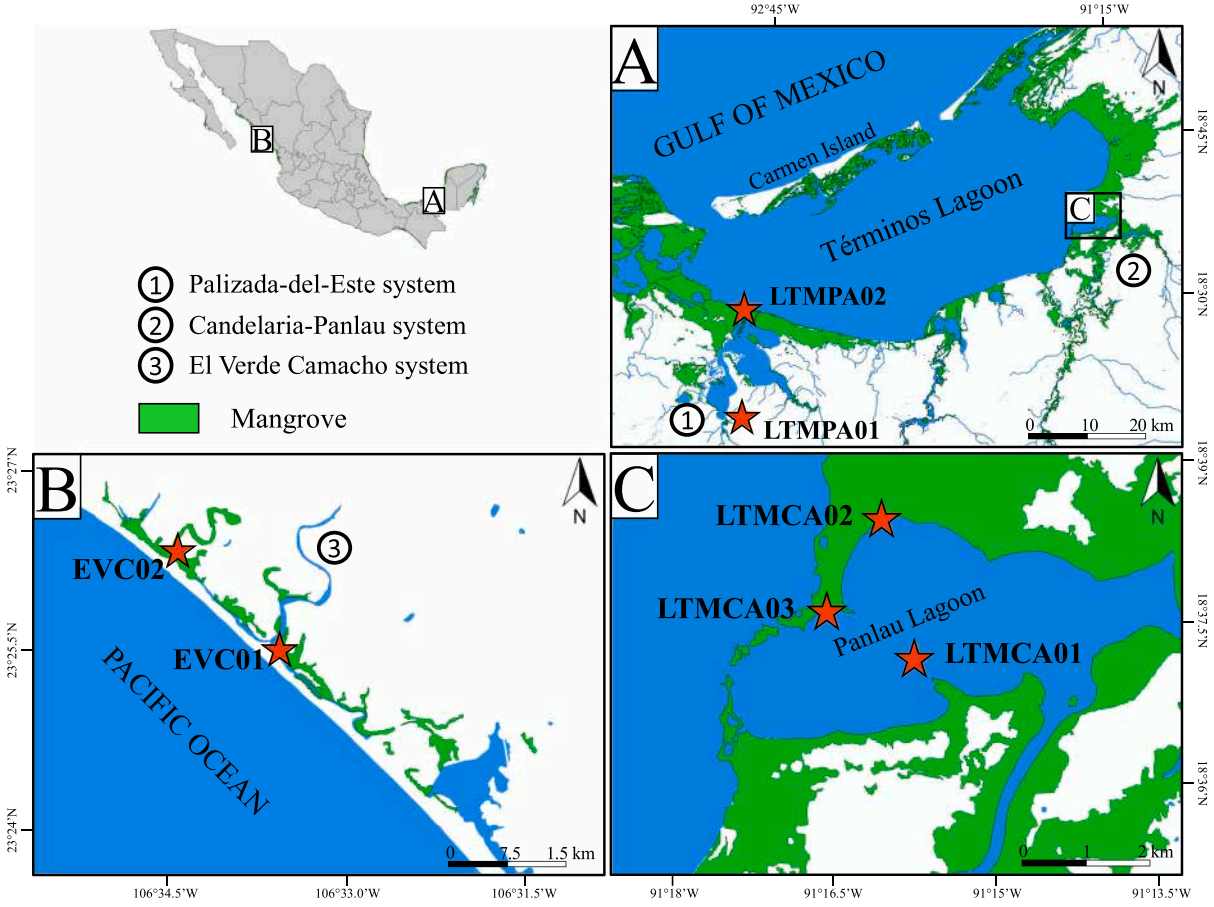

Fig. 1. Location of the seven sediment cores (★) collected in Términos Lagoon (southern Gulf of Mexico) and El Verde Camacho Lagoon (entrance of the Gulf of California).

hydrology, sedimentary and geomorphic settings) that influence C_{org} accumulation and degradation, and therefore complicate the understanding of C_{org} dynamics and their implications at regional and global scales (Breithaupt and Steinmuller, 2022; Rosentreter et al., 2018). Uncertainty persists regarding mangrove responses to climate-induced factors (e.g., droughts, floods, hurricanes) and anthropogenic interventions (e.g., land-use changes, deforestation), with impacts spatially nonuniform worldwide (Macreadie et al., 2019).

The stable isotopic composition of carbon ($\delta^{13}C$) and nitrogen ($\delta^{15}N$) and the C:N ratio are valuable indicators for discerning the origin of C_{org} stored in mangrove sediments (e.g., Bouillon et al., 2003, 2008; Kusumaningtyas et al., 2019), which enable the interpretation of the variability of C_{org} accumulation and the effectiveness of C_{org} storage. Unlike linear mixing models, which use a fixed isotopic composition for each source, Bayesian tracer mixing models account for the potential variability within isotopic composition data (i.e., mixtures and sources) and effectively propagates the associated uncertainties, resulting in more realistic predictions within the estimated likelihood (Stock and Semmens, 2016a). The Bayesian mixing model MixSIAR is the most recent advancement among mixing models. It builds upon years of investigation on mixing models, incorporating features from previous models, such as MixSIR (Moore and Semmens, 2008) and SIAR (Parnell et al., 2013, 2010), and introducing novel user-specified parameters (e.g., a priori information, categorical and continuous covariates) to improve accuracy and reliability in estimating source-to-mixture proportions (Stock et al., 2018). It has been successfully employed to investigate food webs and trophic structures (e.g., Soria-Barreto et al., 2021) and carbon sourcing in river catchments (e.g., Menges et al., 2020). In mangrove sediments, carbon sources may exhibit notable spatial and temporal variations (e.g., Gonneea et al., 2004), however the flexibility and repeatability of MixSIAR enables the exploration of most realistic predictions by creating a framework of different Bayesian mixing models and incorporating customizable options.

In a previous study, Jupin et al. (2023) assessed the temporal trends of sediment accumulation rates over the past century in seven lead-210 (^{210}Pb) dated sediment cores collected in mangrove areas in two contrasting coastal lagoons of Términos Lagoon (TL) in the southern Gulf of Mexico and El Verde Camacho Lagoon (EV) in the entrance of the Gulf of California. The study lagoons exhibited contrasting characteristics, as TL experienced higher rainfall rates, river discharges, and economic development than EV. Consistent exponential trends in mass accumulation rates (MAR) toward the present were observed across all cores, with an acceleration noted since the 1950s. These trends were attributed to continental soil erosion induced by land-use change and sea-level rise.

The present study, based on the ^{210}Pb-derived chronology previously established for the seven sediment cores from TL and EV mangroves, provides new insights on changes in source contributions, burial rates, and stocks of sedimentary C_{org} over the past century, by using Bayesian tracer mixing model MixSIAR and standardized methods. The main questions addressed in this study were: i) how do the ranges of C_{org} burial rates and stocks in the study areas compare to each other and with other mangrove ecosystems worldwide? ii) have changes in sediment and C_{org} sources influenced the temporal trends (~100 years) of C_{org} burial rates and stocks in the study sites? Over the past century, an overall decline in C_{org} concentration, burial rates, and stocks was hypothesized as a result of increasing land-use changes, mangrove cover loss, and sediment inputs, which would favor the accumulation of allochthonous C_{org}.

2. Study sites

2.1. Términos Lagoon

Términos Lagoon (TL), in the southern Gulf of Mexico, is Mexico's most extensive coastal lagoon (Yáñez-Arancibia and Day, 1982;

Table 1
Main characteristics of the study sites in the southern Gulf of Mexico and the entrance of the Gulf of California.

Characteristics	Palizada-del-Este	Candelaria-Panlau	El Verde Camacho	Reference
Sedimentary setting[a]	Terrigenous	Carbonate	Terrigenous	Ortiz-Pérez and de la Lanza-Espino (2006); Rendón-Von Osten et al. (2006); Medina-Gómez et al. (2015)
Geomorphic class	Fluvial-Lagoon	Fluvial-Lagoon	Lagoon	
Climate regime (type)	Warm, humid (Am (f))	Warm, sub-humid (Aw2 (w))	Very warm, semiarid (BW(h')w (e))	García (1973); Briseño-Dueñas (2003); Ochoa (2003); CONAGUA (2015); Ramos-Miranda and Villalobos-Zapata (2015)
Mean annual precipitation (mm yr^{-1})	1750	1400	750	
Mean annual temperature (°C)	27	27	25	
Mean annual salinity	4	15	14	
River name	Palizada	Candelaria + Mamantel	Quelite	Bach et al. (2005); Fichez et al. (2017)
Annual mean discharge (10^9 m^3 yr^{-1})	9.1	1.6 + 0.16	0.11	
Basin (km^2)	40,000	7160 + 520	835	
Annual mangrove loss (ha yr^{-1})[b]	60	16	1	CONABIO (2013, 2021)
Total mangrove loss (%)[b]	21	9	27	

[a] Sedimentary settings were defined based on Breithaupt and Steinmuller (2022). Terrigenous settings indicate externally sourced sediments; carbonate settings indicate locally formed sediments through calcareous processes.
[b] Mangrove loss was estimated over the 1970–2020 period based on CONABIO (2013, 2021).

Contreras-Ruiz-Esparza et al., 2014). It is characterized by a permanent water exchange with the Gulf of Mexico via the inlets on opposite sides of Carmen Island (Fig. 1). The Palizada-del-Este (PDE) in the western zone and the Candelaria-Panlau (CP) in the eastern zone of TL were previously defined as fluvial-lagoon subsystems (e.g., Rendón-Von Osten et al., 2006; Medina-Gómez et al., 2015). Details regarding the main geological, climatic, and hydrologic characteristics of PDE and CP are detailed in Table 1. TL has experienced significant land-use changes due to the population growth of El Carmen Municipality, mainly driven by shrimp and oil industries since the 1950s and 1970s, respectively. The construction of canal networks, pipelines, and roads has negatively impacted wetland areas, particularly the PDE system (Ochoa, 2003). In the basins of the main rivers that discharge into TL, the gradual conversion of wetlands and primary forests into urban and agricultural zones accounted for a forest cover loss of ~31 % between 1974 and 2001 (Cotler-Ávalos, 2010; Soto-Galera et al., 2010).

Previous studies about C_{org} accumulation in TL mangrove sediments include C_{org} burial rates in channels at southeastern Carmen Island (53 and 65 g m^{-2} yr^{-1}, Gonneea et al., 2004) and C_{org} stocks in the southeast of Carmen Island (12–222 Mg ha^{-1}, Cerón-Bretón et al., 2011) and in the Pom-Atasta System northwest of TL (80–236 Mg ha^{-1}, Guerra-Santos et al., 2014). However, C_{org} stocks were obtained from undated sediment cores (30 or 60 cm long), so they were likely not formed during comparable periods. Presently, studies examining C_{org} sources, burial rates, and stocks in mangrove areas of TL and its subsystems are scarce, especially using ^{210}Pb-dated sediment cores.

2.2. El Verde Camacho Lagoon

El Verde Camacho Lagoon (EV) is a 47 ha internal coastal barrier lagoon (Fig. 1, Table 1). It receives marine water inputs during the rainy season (June to October) when the sandbar breaks due to the higher elevation of tides, the larger Quelite River discharge, and occasional tropical storms and hurricanes (Flores-Verdugo et al., 1995). The beach and wetlands in EV are relatively well preserved; however, native vegetation loss has been promoted by the development of tourism, aquaculture facilities, and human settlements in the Mazatlán municipality (Briseño-Dueñas, 2003). The mean annual deforestation rate in Mazatlán was estimated at 0.36 % between 1993 and 2011 (Monjardín-Armenta et al., 2017). During the dry season, ~90 % of C_{org} inputs to the EV come from mangrove leaf defoliation, whereas during the rainy season, C_{org} is exported to the ocean through the Quelite River and tidal currents (Flores-Verdugo et al., 1995, 1987; González-Farías and Mee, 1988). To our knowledge, there are no previous investigations on sedimentary C_{org} burial rates and stocks in EV mangroves.

3. Methods

3.1. Sampling, dating, and analysis

3.1.1. Core sampling and sediment dating

Sampling and ^{210}Pb dating of the cores are detailed in Jupin et al. (2023). Briefly, sampling sites were selected by analyzing mangrove distribution in the study areas using aerial photographs and satellite images (CONABIO, 2021, 2013) to identify unchanged mangrove areas over the past 50 years. Two sediment cores were to be retrieved at each study site to guarantee duplicate samples and high-quality data. However, the presence of fine roots at one sampling site within the CP system prompted the collection of an additional core from a third sample site to ensure accurate ^{210}Pb dating of the cores. Ultimately, a total of seven sediment push cores (PVC tubes of 10 cm internal diameter, 1 m length) were collected in 2021 in undisturbed flat areas within fringe mangrove communities with similar topographic features and species composition for site comparison (Table 2). All cores yielded positive results upon processing, enabling the valuable reconstruction of local variations in C_{org} burial rates and stocks, especially in regions where data are notably scarce and absent from the global database. The cores were extruded and sectioned at 1 cm intervals, and the samples were lyophilized and ground to powder with porcelain mortar and pestle (except those for grain size analysis). Analytical results are expressed on a dry weight basis.

For core dating, ^{210}Pb, ^{226}Ra, and ^{137}Cs activities were determined by low background gamma-spectrometry as described in Díaz-Asencio et al. (2020). The Constant Flux (CF) model, which assumed a constant flux of atmospheric ^{210}Pb to the sediment surface, was used to obtain the age models and the mass accumulation rates (MAR; g cm^{-2} yr^{-1}) of the cores (Sanchez-Cabeza and Ruiz-Fernández, 2012). Dating uncertainties were estimated using Monte Carlo simulation with 30,000 iterations (Sanchez-Cabeza et al., 2014). To strengthen confidence in the ^{210}Pb chronologies, ages derived from CF model were cross-compared to those generated by Bayesian ^{210}Pb age-depth using the package rPlum (Blaauw et al., 2021). The maximum of ^{137}Cs activities and the identification of meteorological events were used to corroborate the ^{210}Pb chronologies in the sediment cores.

3.1.2. Element and isotopic composition

Concentrations of organic carbon (C_{org}) and total nitrogen (N) and isotopic composition of C ($\delta^{13}C$) and N ($\delta^{15}N$) were measured with an Elemental Analyzer Flash 2000 HT coupled to an Isotope Ratio Mass Spectrometer Delta V Advantage (EA-IRMS) from Thermo Fisher Scientific. For C_{org} and $\delta^{13}C$ determination, carbonates were removed from bulk sediment using HCl (10 %) before analyses. N and $\delta^{15}N$ were determined on bulk sediments. Isotope ratios were reported in the conventional delta (δ in ‰) notation relative to Pee Dee Belemnite (PDB) carbonate standard and atmospheric N_2 (air), respectively.

Table 2
Sampling data of mangrove sediment cores from Términos Lagoon (southern Gulf of Mexico) and El Verde Camacho Lagoon (entrance of the Gulf of California).

System	Core collection date	Core name	Length (cm)	Coordinates (latitude N; longitude W)	Dominant mangrove species	Age (dated period)	MAR (g cm^{-2} yr^{-1})
Términos	Lagoon						
PDE	2021-02-11	LTMPA01	69	18°20.3319; 91°47.7541	Rm	102 (1918–2020)	0.25 ± 0.03
		LTMPA02	47	18°29.0131; 91°47.7362	Rm; Ag; Lr	120 (1900–2020)	0.27 ± 0.01
CP	2021-02-12	LTMCA01	66	18°37.1903; 91°16.0722	Rm; Ag; Lr	118 (1902–2020)	0.24 ± 0.01
		LTMCA02	64	18°38.4186; 91°16.3408	Rm; Lr	117 (1903–2020)	0.14 ± 0.01
		LTMCA03	76	18°37.6450; 91°16.7640	Rm; Lr	112 (1908–2020)	0.20 ± 0.07
El Verde	Camacho Lagoon						
EV	2021-07-06	EVC01	65	23°42.384; 106°55.820	Rm; Lr	90 (1931–2021)	0.43 ± 0.20[a]
		EVC02	69	23°43.893; 106°57.387	Rm	118 (1903–2021)	0.43 ± 0.08[a]

PDE: Palizada-del-Este; CP: Candelaria-Panlau; EV: El Verde Camacho.
Rm: *Rhyzophora mangle*; Lr: *Laguncularia racemose*; Ag: *Avicennia germinans*.
[a] Mass accumulation rates (MAR) were calculated excluding maxima attributed to meteorological events. See the text for an explanation.

Element composition (Al, Ca, Ti, Na) was determined using an Inductively Coupled Plasma – Mass Spectrometer (ICP-MS) Agilent 7500 cx, for which aliquots of ~25 mg of sediments were previously acid-digested (2 mL HF 40 % Normapure, 1 mL $HClO_4$ 70–72 % Merck, 2 mL HNO_3 65 % Normapure) on a hot-plate (150 °C for six days) (Carter et al., 2015). The annual fluxes of Al and Ca were calculated by multiplying their respective element concentrations by ^{210}Pb-derived MAR. They served as indicators of terrestrial inputs originating from river basins with terrigenous (PDE and EV) and carbonate (CP) settings (Table 1). The Al/Ti ratios were used to discern variations in mineralogical composition or input sources within the sediment cores and the Na/Al ratios were used as a proxy for assessing marine influence and paleosalinity (Croudace and Rothwell, 2015).

3.1.3. Quality control and quality assurance

Analysis of certified reference materials provided results within the reported range of the recommended values, including IAEA-384 for gamma-ray spectrometry, MESS-3 for trace elemental analysis, and HOS for EA-IRMS. The analytical precision was determined through the coefficient of variation (CV (%) = standard deviation/mean value × 100) from replicate analysis of a single sample ($n = 6$); CVs were <5 % for ^{210}Pb, ^{137}Cs, and elemental determination, and <0.35 % for δ^{13}C and δ^{15}N.

3.2. Data treatment

3.2.1. Mixing model setup for organic carbon sources

The fractions of different sources contributing to sedimentary C_{org} in the cores were estimated using the Bayesian isotope mixing model MixSIAR (Stock and Semmens, 2016a; Stock et al., 2018). The mixture data were the δ^{13}C and δ^{15}N values ($n = 327$) from the seven study cores (Fig. 2). Reference δ^{13}C and δ^{15}N values for the main sources were obtained from previous studies (Table S1, in Supplementary Material) in the study sites or their vicinity. The reference source values were averaged, and the means, along with their standard deviations (mean ± SD), were utilized in the mixing model (Stock and Semmens, 2016b). Primary sources included: i) mangrove detritus, mainly composed of mangrove leaves, and considered the primary in situ C_{org} source; ii) particulate organic matter of terrestrial origin transported by rivers; and iii) phytoplankton, as an indicator of marine-derived C_{org} for EV and C_{org} originating from the TL for PDE and CP.

Assumptions of the model included that all sources were known and quantified, mixture data were conserved through the mixing process and mixture and source values were fixed (Stock and Semmens, 2016b; Stock et al., 2018). The MixSIAR parameters can include a discrimination factor to address variation between values found in the mixture and those from the sources. In this study, this factor was considered as negligible and defined as '0' in the models, on the assumptions that diagenesis had a limited impact on the stable isotope composition of carbon and nitrogen (Cifuentes et al., 1996; Kusumaningtyas et al., 2019; Meyers, 1997) and mixing values found in sediments cores, representing different ages, were comparable to contemporary published source values (Douglas et al., 2022; Menges et al., 2020). Those assumptions were supported by the minimal differences observed in δ^{13}C and δ^{15}N values between preserved mangrove leaves and detritus from published values (Gonneea et al., 2004; Medina-Contreras et al., 2023; Sepúlveda-Lozada et al., 2017, 2015). The model setup included as categorical factors the core name per site and decadal periods (e.g., 0–10 years). Sections older than 100 years were categorized as ">100 years". The prior was defined as an "uninformative" prior with $\alpha = c(1,1,1)$ to indicate equal weighting for each source without any prior information influencing the model. MixSIAR models were executed using Markov Chain Monte Carlo (MCMC). Results were summarized as boxplots of the posterior density distributions, i.e., mean, standard deviation, and Bayesian 5–95 % credible intervals of each categorical factor.

C_{org} sources in mangrove sediments may vary spatially and temporally (Adame and Fry, 2016; Gonneea et al., 2004). A comprehensive literature review was conducted to identify studies providing source values that best represented the study sites and addressed minor uncertainty. The utilization of local or regional reference values from published data, while occasionally limited for certain sites, proved effective in minimizing uncertainty and enhancing consistency in mixing models compared to global means. To guarantee accurate estimation of the posterior distributions, a MCMC run (selected as "long" within the software) consisting of 300,000 iterations was executed. The model convergence was assessed through the Gelman-Rubin and Geweke tests (for more detail, see Stock and Semmens, 2016b). Changes in C_{org} sources were further associated with temporal variability of additional indicators, such as the C:N ratio, elemental composition, and environmental data (e.g., precipitation, river discharge, and land-use change).

3.2.2. Organic carbon burial rates and stocks

C_{org} burial rates (g m^{-2} yr^{-1}) were calculated as the product of C_{org} concentrations and ^{210}Pb-derived MAR at each core section (Ruiz-Fernández et al., 2018b). MAR maxima in EV cores were attributed to meteorological events (Jupin et al., 2023) and excluded from the calculations. C_{org} stocks (Mg ha^{-1}), which represent the current amount of C_{org} stored within the sediment that might be released as CO_2 emissions if mangrove sediments were disturbed, were calculated as the sum, from the core surface to the bottom, of the product of the concentration of C_{org}, the dry bulk density, and the thickness of each section (Howard et al., 2014). For comparison purposes, C_{org} stocks in all cores were calculated up to 50 cm depth (C_{org} $stock_{\text{-}50cm}$). For sediment cores displaying constant C_{org} concentrations in their bottom sections (i.e., LTMPA02, LTMCA03, EVC01, Fig. 3), suggesting negligible C_{org} degradation over time, C_{org} stocks were extrapolated to 1 m depth (C_{org} $stock_{\text{-}1m}$) by extending the known average C_{org} stock from the bottom sections up to the depth of 1 m, assuming uniformity of C_{org} stocks in the intervening layers (Ruiz-Fernández et al., 2018a). The resulting values of C_{org} $stock_{\text{-}1m}$ were compared with the global database (Atwood et al., 2017), exclusively considering information from countries with available field data (i.e., excluding country estimations derived from calculations based on the global mean C_{org} $stock_{\text{-}1m}$). The temporal variation of C_{org} stocks was calculated per decade ($stock_{\text{-}10yr}$), century (C_{org} $stock_{\text{-}100yr}$), as well as for the periods 1900–1950 (C_{org} $stock_{\text{-}1900\text{-}1950}$) and 1950 to sampling date (C_{org} $stock_{\text{-}1950\text{-}2021}$).

The CO_2 equivalent (CO_{2eq}, in Mg ha^{-1}) emissions, in case of significant C_{org} stock loss, were calculated by multiplying the C_{org} stocks (at 50 cm or 1 m) by the conversion factor 3.67 (i.e., the ratio of C to CO_2 molecular weights) (Howard et al., 2014). Potential annual CO_{2eq} emissions from mangrove losses were estimated by multiplying the mean CO_{2eq} per site by the mean yearly mangrove habitat loss calculated for 1970–2020 (CONABIO, 2013, 2021). The uncertainties of C_{org} stocks, burial rates, and CO_{2eq} emissions were estimated by quadratic uncertainty propagation (Cuellar-Martinez et al., 2019). The uncertainties of C_{org} stocks by depth (1–6 %) were low owing to the precision of the C_{org} measurements, whereas the larger uncertainties in 10 years-C_{org} stocks (7–32 %) were primarily caused by the MAR uncertainties, associated with the dating computation.

3.3. Statistical analysis

The Shapiro-Wilk test confirmed that the variables in the dataset were not normally distributed. The distribution of variable ranks among cores was compared using the non-parametric Kruskal-Wallis one-way analysis of variance (ANOVA) and the post-hoc Dunn test. Associations between variables were assessed through a Spearman correlation analysis followed by a Student's *t*-test. All tests were performed at a 95 % confidence level.

Table 3
Elemental concentration and isotopic composition of C and N, C:N ratio, and burial rates in mangrove sediment cores from Términos Lagoon (southern Gulf of Mexico) and El Verde Camacho Lagoon (entrance of the Gulf of California).

Core	Statistics	C_{org} (%)	N (%)	$\delta^{13}C$ (‰)	$\delta^{15}N$ (‰)	C:N ratio	C_{org} burial rate (g m^{-2} yr^{-1})
Términos	Lagoon						
LTMPA01	Min	1.69 ± 0.02	0.112 ± 0.002	−29.94 ± 0.06	3.7 ± 0.1	14.6 ± 0.3	25 ± 13
	Max	10.8 ± 0.1	0.540 ± 0.010	−26.98 ± 0.06	5.1 ± 0.1	29.4 ± 0.9	430 ± 170
	Mean	3.90 ± 0.05	0.222 ± 0.004	−28.09 ± 0.06	4.3 ± 0.1	19.3 ± 0.4	140 ± 65
LTMPA02	Min	0.97 ± 0.03	0.078 ± 0.002	−28.4 ± 0.1	4.3 ± 0.1	12.5 ± 0.4	4 ± 2
	Max	4.66 ± 0.04	0.275 ± 0.003	−26.4 ± 0.1	6.3 ± 0.2	22.9 ± 0.5	210 ± 30
	Mean	1.91 ± 0.03	0.154 ± 0.002	−27.0 ± 0.1	5.2 ± 0.2	15.7 ± 0.5	66 ± 16
LTMCA01	Min	1.50 ± 0.03	0.109 ± 0.001	−27.9 ± 0.1	4.2 ± 0.3	13.6 ± 0.4	11 ± 5
	Max	14.3 ± 0.1	0.531 ± 0.007	−25.9 ± 0.1	6.5 ± 0.3	35.8 ± 0.8	490 ± 50
	Mean	3.13 ± 0.04	0.211 ± 0.004	−26.7 ± 0.1	5.2 ± 0.3	20.0 ± 0.5	110 ± 23
LTMCA02	Min	12.20 ± 0.2	0.386 ± 0.006	−29.6 ± 0.1	1.6 ± 0.3	18.9 ± 0.6	81 ± 16
	Max	32.0 ± 0.5	1.570 ± 0.020	−26.1 ± 0.1	2.7 ± 0.3	69.0 ± 2.0	800 ± 84
	Mean	24.6 ± 0.4	1.090 ± 0.020	−28.5 ± 0.1	2.2 ± 0.3	26.5 ± 0.8	400 ± 40
LTMCA03	Min	2.53 ± 0.04	0.163 ± 0.005	−27.7 ± 0.1	4.03 ± 0.05	8.9 ± 0.3	24 ± 13
	Max	11.7 ± 0.7	0.690 ± 0.020	−25.90 ± 0.06	6.44 ± 0.05	26.0 ± 1.0	290 ± 30
	Mean	4.4 ± 0.3	0.315 ± 0.009	−26.72 ± 0.08	5.0 ± 0.3	14.0 ± 1.0	120 ± 24
El Verde	Camacho	Lagoon					
EVC01	Min	0.65 ± 0.04	0.032 ± 0.001	−26.51 ± 0.03	6.2 ± 0.1	10.9 ± 0.3	12 ± 13
	Max	4.56 ± 0.05	0.244 ± 0.005	−23.94 ± 0.03	9.3 ± 0.2	25.0 ± 2.0	270 ± 160[a]
	Mean	1.53 ± 0.04	0.010 ± 0.002	−24.9 ± 0.1	8.0 ± 0.1	17.5 ± 0.9	86 ± 95[a]
EVC02	Min	1.63 ± 0.07	0.100 ± 0.004	−27.59 ± 0.03	2.9 ± 0.3	14.8 ± 0.6	33 ± 22
	Max	8.90 ± 0.07	0.396 ± 0.007	−24.8 ± 0.2	7.5 ± 0.3	26.0 ± 1.0	800 ± 240[a]
	Mean	3.17 ± 0.05	0.190 ± 0.005	−25.8 ± 0.1	6.0 ± 0.3	19.4 ± 0.8	190 ± 30[a]

C_{org}: organic carbon; N: total nitrogen; Min: minimum; Max: maximum.
[a] C_{org} burial rates were calculated excluding maxima of mass accumulation rates attributed to meteorological events. See the text for an explanation.

4. Results

4.1. Organic carbon and total nitrogen concentration and trends

The C_{org} and N concentrations were highest ($p < 0.05$) in core LTMCA02 and lowest in LTMPA02, but comparable among the rest of the TL cores (LTMCA02 > LTMCA01 = LTMCA03 = LTMPA01 > LTMPA02; Table 3). In EV, EVC02 C_{org} concentrations were higher ($p < 0.05$) than in EVC01. Significant correlations ($p < 0.05$) between C_{org} and N concentrations ($r > 0.90$ in PDE; $r > 0.86$ in CP; $r > 0.90$ in EV) were observed in the sediment cores, indicating that N content in the sediment was predominantly originated from organic sources. C_{org} and N concentrations gradually increased from the oldest sections to the present (Fig. 3).

4.2. Organic carbon sources

4.2.1. C:N ratios and C_{org} and N isotope composition

In TL, C:N ratios and $\delta^{13}C$ and $\delta^{15}N$ values were highest ($p < 0.05$) in LTMCA02 and lowest in LTMPA02, but comparable in the other cores LTMCA01, LTMPA01, and LTMCA03 (Table 3). In EV, the cores EVC02 and EVC01 had comparable C:N ratios but different $\delta^{13}C$ and $\delta^{15}N$ (EVC01 > EVC02). The C:N ratios in all cores generally decreased from the older sections to the last few decades, followed by an increase observed in the period 2000–2021 (Fig. 3). In the TL cores, $\delta^{13}C$ values generally decreased toward the most recent sections, whereas $\delta^{15}N$ profiles showed high variability. In EV cores, $\delta^{13}C$ and $\delta^{15}N$ values increased from older sections to the early 2000s and then decreased to the present time.

Table 4
Storage and source contributions of organic carbon in mangrove sediment cores from Términos Lagoon (southern Gulf of Mexico) and El Verde Camacho Lagoon (entrance of the Gulf of California).

Core	Stock (Mg ha^{-1})						Mean contribution of C_{org} sources (%)		
		Over the 1900–1950 period	Over the 1950–2021 period	Over the past 100 years	To 50 cm depth	Extrapolated to 1 m depth	Mangrove detritus	Fluvial	Phytoplankton
Términos	Lagoon								
LTMPA01	C_{org}	19 ± 3	92 ± 3	105 ± 1	131 ± 1	na	55	32	13
	CO_{2eq}	72 ± 9	337 ± 11	385 ± 4	478 ± 3	na			
LTMPA02	C_{org}	6.4 ± 0.3	43 ± 1	47.8 ± 0.5	85 ± 1	137 ± 2	19	64	17
	CO_{2eq}	24 ± 1	158 ± 2	176 ± 2	311 ± 2	501 ± 6			
LTMCA01	C_{org}	8.0 ± 0.5	69 ± 1	74.2 ± 0.9	106 ± 1	na	14	71	15
	CO_{2eq}	29 ± 2	251 ± 4	272 ± 3	387 ± 3	na			
LTMCA02	C_{org}	50 ± 1	254 ± 1	276.1 ± 0.9	255 ± 2	na	84	3	13
	CO_{2eq}	182 ± 3	899 ± 4	1013 ± 3	935 ± 6	na			
LTMCA03	C_{org}	15.2 ± 0.4	86 ± 1	95.4 ± 0.6	137 ± 2	241 ± 4	24	65	11
	CO_{2eq}	56 ± 1	316 ± 2	350 ± 2	502 ± 6	883 ± 13			
El Verde	Camacho	Lagoon							
EVC01	C_{org}	16 ± 2	70 ± 3	79 ± 3	98 ± 1	182 ± 1	21	78	1
	CO_{2eq}	58 ± 6	258 ± 12	291 ± 10	358 ± 3	666 ± 4			
EVC02	C_{org}	36 ± 1	113 ± 2	139 ± 3	114 ± 1	na	43	41	16
	CO_{2eq}	133 ± 4	414 ± 7	512 ± 10	429 ± 3	na			

C_{org}: organic carbon; CO_{2eq}: carbon dioxide equivalent emissions in case of sediment disturbances in the sampling sites. na = not available. See the text for an explanation.

4.2.2. Mixing models

The relative contribution of the primary sources of C_{org} to the sediments varied both geographically and temporally, with the predominance of autochthonous mangrove detritus in LTMPA01 and LTMCA02, and the predominance of allochthonous fluvial C_{org} in LTMPA02, LTMCA01, and LTMCA03 (Table 4). In EV cores, allochthonous fluvial C_{org} predominated in EVC01, while EVC02 sediments exhibited a combination of mangrove detritus and fluvial C_{org}. Only a minor contribution of phytoplankton-derived C_{org} was observed in the cores (Table 4).

In the sediment cores, both fluvial and mangrove C_{org} sources generally increased by 5–41 % and by 5–32 %, respectively, from before the 1900s to the 2000s (Fig. 4), except in LTMCA02 where fluvial C_{org} remained minimal (1.2–4.4 %). After the 2000s, contributions of mangrove detritus increased by 18–20 % in PDE cores, 5–6 % in CP cores, and 19–27 % in EV cores. Simultaneously, contributions of phytoplankton-derived C_{org} decreased by 12–32 % in all cores, except for EVC01, where contributions remained consistently low (0.5–3.6 %). The Bayesian 5–95 % credible intervals for C_{org} sources in the CP cores during the period 1961–1981 were notably wider compared to other time intervals. In LTMCA01 and LTMCA03, this period revealed an increase of 11–14 % in the contribution of lagoon phytoplankton-derived C_{org}, along with a simultaneous reduction of 21 % in the contribution of fluvial C_{org}, relative to the preceding decade. The core LTMCA02 recorded a 6 % increase in lagoon phytoplankton-derived C_{org}, with no concurrent increase in fluvial C_{org}.

4.2.3. Indicators of terrestrial and marine inputs

In the post-1950s segment, the Al and Ca concentrations and the Al/Ti ratios generally increased in all cores, whereas the Na/Al ratios decreased, particularly in cores LTMPA01, LTMCA01, LTMCA03, and EVC01.

4.3. Organic carbon burial rates and stocks

The order of C_{org} burial rates in TL cores was LTMCA02 > LTMCA01 = LTMCA03 = LTMPA01 > LTMPA02, whereas in EV cores, they were higher ($p < 0.05$) in EVC02 than in EVC01 (Table 3). Both C_{org} stock$_{\text{-10yr}}$ and burial rates increased steadily from the early 1900s to the present in all cores, although the pace accelerated from the ~1950s onward (Figs. 4 and 5).

C_{org} stock$_{\text{-50cm}}$ values were higher in CP than other systems, whereas those of C_{org} stock$_{\text{-1m}}$ (where available) varied considerably (LTMCA03 > LTMPA01 > EVC01) (Table 4). The lowest C_{org} burial rates were observed in the cores LTMPA02 and EVC02 that were collected in mangrove areas closer to river mouths. In contrast, the highest C_{org} burial rates were found in cores LTMCA02 and LTMPA01 collected farther from the direct river influence (Fig. 1). C_{org} stocks$_{\text{-1950-2021}}$ were ~12–32 % higher than C_{org} stocks$_{\text{-1900-1950}}$ (Table 4), contributing to 80–92 % of the total stocks accumulated between 1900 and 2021 in each core. The C_{org} stocks$_{\text{-10yr}}$ in core LTMCA02 were the highest, ranging from ~2 to 6-fold higher than in the other cores (Fig. 4). The potential CO_{2eq} emissions in case of sediment disturbances reached 311–935 Mg ha^{-1} at 50 cm depth and 501–883 Mg ha^{-1} at 1-meter depth (where available) (Table 4). Potential annual CO_{2eq} emissions from mangrove losses per site were 30.1 ± 0.4 Tg yr^{-1} in PDE, 14.1 ± 0.2 Tg yr^{-1} in CP, and 0.67 ± 0.01 Tg yr^{-1} in EV.

5. Discussion

5.1. Major sources of organic carbon

The dominant fluvial C_{org} contribution (64–78 %; Table 4) in cores LTMPA02, LTMCA01, LTMCA03, and EVC01 is a common feature in river-influenced mangrove ecosystems, where the allochthonous C_{org} usually represents most of the total contribution (Kusumaningtyas et al., 2019; Sasmito et al., 2020). The relatively minor contribution of phytoplankton-derived C_{org} (1–17 %; Table 4) or seagrass material in all cores suggested a limited influence of the tidal regime onto the C_{org} supply to the sediments, in comparison to the fluvial sources. Seagrass is often considered in the investigation of organic matter sources in mangroves (Gonneea et al., 2004; Sepúlveda-Lozada et al., 2017, 2015) and was initially integrated as a primary source in the mixing models. However, during the preliminary analysis of $\delta^{13}C$ and $\delta^{15}N$ values within the mixing polygon defined by basal sources (Fig. 2; Brett, 2014), the integration of seagrass as a source resulted in mixing data falling outside the polygon, indicating an incorrect or missing source (Stock and Semmens, 2016b), and led to convergence issues in the models. While seagrass may be present in the study sites, it was determined as a minor contributor (<2 %) and therefore was excluded in this study.

The relatively high accumulation of mangrove-derived detritus C_{org} in cores LTMPA01 and LTMCA02 (55 and 84 %, respectively; Table 4) is typical for mangrove ecosystems without significant river or tidal influence, where C_{org} primarily originates from autochthonous sources, such as mangrove leaves and roots (Alongi, 2014). The high contribution of mangrove detritus in the mixing models was aligned with the highest C:N values (29–69; Table 3), corresponding to values generally found in mangroves detritus (20–30 in mangrove leaves and 50–60 in mangrove wood; Lallier-Vergès et al., 1998; Marchand et al., 2005). The uppermost sections of other cores (LTMPA02, EVC01, and EVC02) also showed high C:N values coinciding with lower $\delta^{13}C$ and $\delta^{15}N$ values (Fig. 3) that

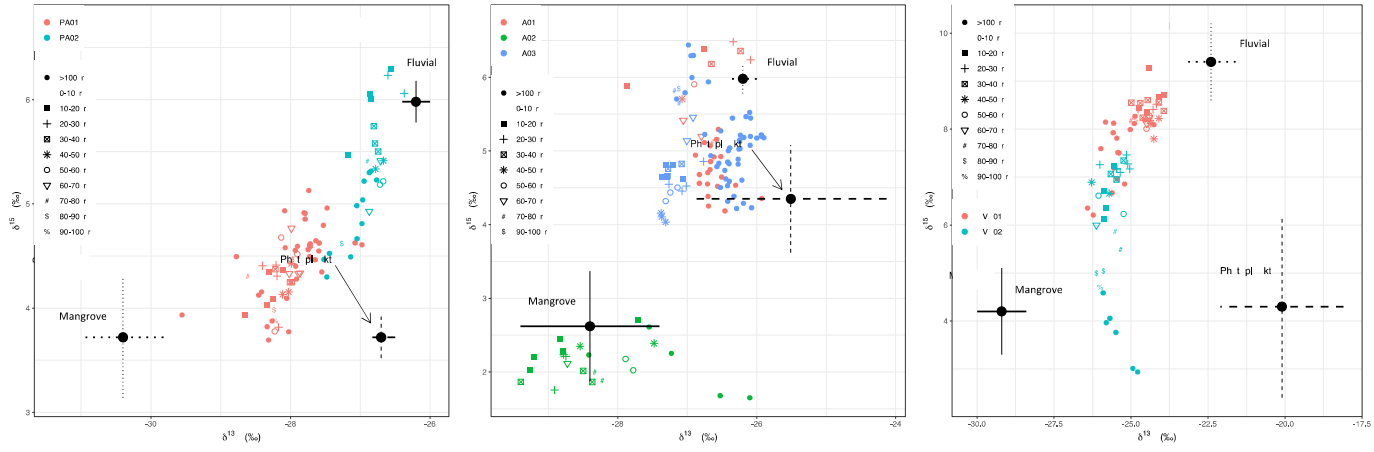

Fig. 2. Values of isotopic composition ($\delta^{13}C$ and $\delta^{15}N$) for mixture (sediment samples) and source data (mangrove: organic matter from mangrove detritus; fluvial: particulate organic matter from river inputs; phytoplankton: lagoon or marine-derived phytoplankton) in sediment cores from Términos Lagoon (southern Gulf of Mexico) and El Verde Camacho Lagoon (entrance of the Gulf of California).

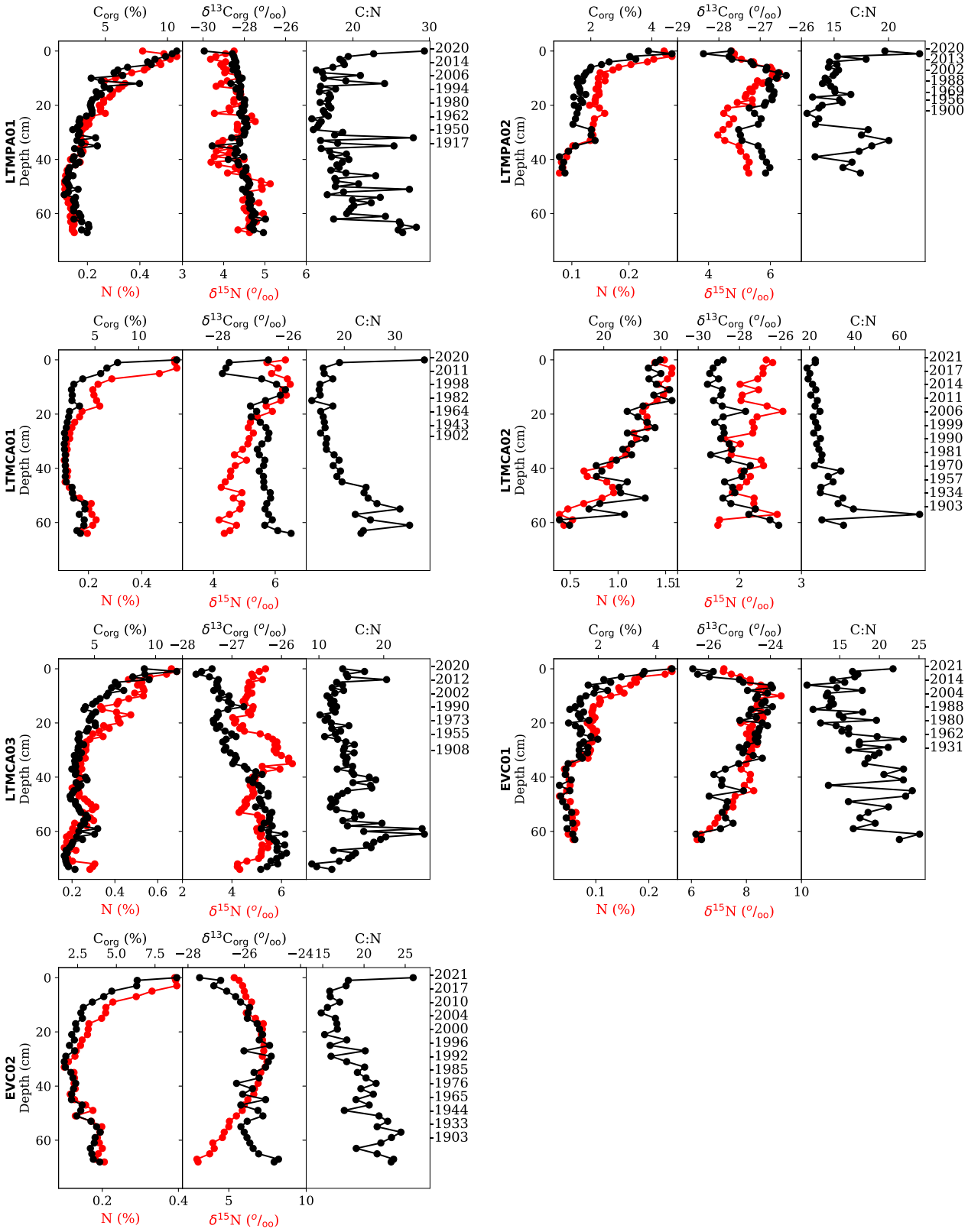

Fig. 3. Elemental concentration and isotopic composition of C and N, and C:N ratios in mangrove sediment cores from Términos Lagoon (southern Gulf of Mexico) and El Verde Camacho Lagoon (entrance of the Gulf of California).

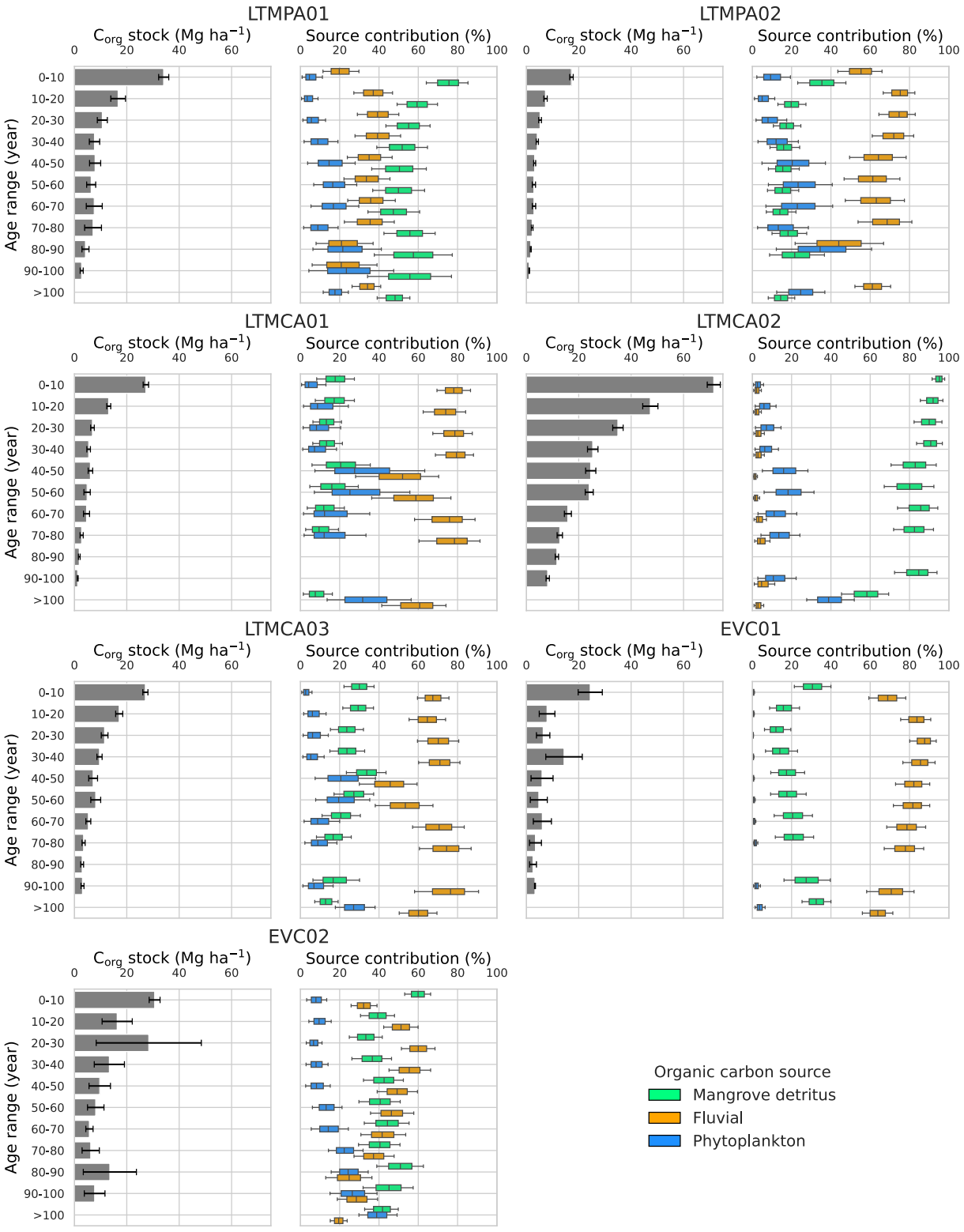

Fig. 4. Temporal variation of organic carbon (C_{org}) stocks and source contribution in mangrove sediment cores from Términos Lagoon (southern Gulf of Mexico) and El Verde Camacho Lagoon (entrance of the Gulf of California).

indicated a higher contribution of mangrove detritus in the most recent period (2021–2011).

The core EVC02 displayed a mixture of fluvial C_{org} and mangrove detritus sources (41 and 43 %, respectively; Table 4), attributed to changes in hydrodynamic conditions influenced by river discharge and storms (Jupin et al., 2023). The impact of storms on C_{org} accumulation can vary considerably, influencing river and tidal currents and sediment dynamics in two ways: i) increasing C_{org} accumulation, facilitated by the trapping of material (e.g., fallen vegetation) derived from storms by mangrove root systems, ultimately resulting in higher sediment accretion and C_{org} accumulation; or ii) causing erosion, C_{org} exportation to the ocean, or mangrove degradation leading to a reduction in productivity

(Pérez et al., 2018; Smoak et al., 2013). EVC02 registered a greater influx of C_{org} during these particular events (Fig. 5), suggesting that its location, farther from the influence of the Quelite River, was prone to C_{org} accumulation during storms, in contrast to EVC01.

5.2. Accumulation of organic carbon in contrasting environmental settings

The mean C_{org} burial rates in PDE (103 ± 47 g m^{-2} yr^{-1}) and EV (138 ± 70 g m^{-2} yr^{-1}) fell within the global mean for mangroves of 139 (120–159) g m^{-2} yr^{-1} (Fig. 6; Breithaupt and Steinmuller, 2022), whereas those in the CP system (210 ± 30 g m^{-2} yr^{-1}) were above the global mean. According to observations from global databases (Breithaupt and Steinmuller, 2022; Woodroffe et al., 2016), mangroves in estuaries or terrigenous settings, which usually receive high contributions of allochthonous C_{org}, tend to exhibit higher C_{org} burial rates compared to mangroves in lagoon or carbonate settings. Conversely, in this study, the highest C_{org} burial rates were found in mangrove areas where the input of autochthonous C_{org} prevailed (LTMCA02 and LTMPA01; Fig. 4) and in mangroves in carbonate settings (CP) compared to those in terrigenous settings (PDE and EV). The comparable C_{org} burial rates among cores from the three subsystems (LTMPA01, LTMCA01, LTMCA03, and EVC02; Table 3) and the significant ($p < 0.05$) differences in C_{org} burial rates among cores from the same study site (e.g., LTMPA01 > LTMPA02 in PDE; LTMCA02 > LTMCA01 and LTMCA02 > LTMCA03 in CP; and EVC02 > EVC01 in EV; Table 3) suggested that, irrespective of the sedimentary settings or geomorphic classes, the spatial distribution of C_{org} burial rates in the study sites was somewhat influenced by local conditions, specific to each core surroundings. The disparity between local and global observations can be attributed to the high local-scale variability commonly observed in mangroves (Jennerjahn, 2020; Pérez et al., 2018), which increases data uncertainties and database biases (e.g., interpolation errors, different timescales, and insufficient data; Sidik and Friess, 2021). The complexity of the processes that affect C_{org} accumulation in mangroves, often overlooked in global-scale analyses, is shown by the wide range of reported C_{org} burial rates in mangrove ecosystems worldwide, which tend to broaden as more data are reported (20–1020 g m^{-2} yr^{-1}, Breithaupt et al., 2012; 2–1749 g m^{-2} yr^{-1}, Breithaupt and Steinmuller, 2022).

The lowest observed C_{org} burial rates in cores LTMPA02 and EVC01 were attributed to their proximity to the river discharge (Fig. 1, Table 3). EVC01 showed a significantly ($p < 0.05$) coarser sediment composition than EVC02, suggesting higher hydrodynamic conditions near the Quelite River mouth (Jupin et al., 2023). Increased hydrodynamic can diminish C_{org} accumulation and storage by regulating the sediments, oxygen, and nutrients supply, thus preventing long-term C_{org} deposition through resuspension processes and promoting aerobic decomposition of sedimentary C_{org} (Allais et al., 2024; Kusumaningtyas et al., 2019). In particular, EVC01 was likely influenced by the seasonal export of in situ C_{org} to the ocean by the Quelite River, occurring during the rainy season (Flores-Verdugo et al., 1995), which would explain its lower proportion of mangrove detritus compared to EVC02 (Table 4). Although the TL cores exhibited comparable grain size distributions (Jupin et al., 2023), runoff in the surroundings of LTMPA02 may have promoted the flushing of suspended sedimentary matter out of the lagoon, promoting export rather than accumulation of autochthonous C_{org} (Bouillon et al., 2003).

5.3. Storage of organic carbon in contrasting environmental settings

At a comparable core depth, the C_{org} $stock_{-50cm}$ values for each mangrove area (PDE: 108 ± 1 Mg ha^{-1}; CP: 166 ± 2 Mg ha^{-1}; EV: 106 ± 1 Mg ha^{-1}; Table 4) were similar to the range found in anthropized mangrove ecosystems of South Australia (87–120 Mg ha^{-1}; Lavery et al., 2019) and pristine mangrove ecosystems in Indonesia (62 ± 10 to 180 ± 82 Mg ha^{-1}; Sasmito et al., 2020), but might be lower than values estimated for Mexican mangrove ecosystems from the southern Mexican Pacific (180 Mg ha^{-1}), the Gulf of Mexico (210 Mg ha^{-1}) and Yucatán (360 Mg ha^{-1}) (Herrera-Silveira et al., 2016), although this comparison is limited because the uncertainties of such values are unavailable. Among cores with available C_{org} $stock_{-1m}$ (Table 4), only that of LTMCA03 (241 ± 4 Mg ha^{-1}) was comparable to the global mean estimate of 251 (200–302) Mg ha^{-1} and the mean estimate for Mexico of 370 ± 176 Mg ha^{-1} (Fig. 7; Atwood et al., 2017). The higher C_{org} stocks (Table 4) were found in cores with higher C_{org} burial rates (Table 3) and sourced from mangrove detritus (Fig. 4), suggesting an efficient preservation of the accumulated autochthonous C_{org}. The C_{org} stocks at 50 cm and 1 m depth were highest in CP and were comparable between EV (North Pacific) and PDE (Gulf of Mexico). This contrasted with the regional pattern previously observed in Mexico (Herrera-Silveira et al., 2020), which showed a lower mean C_{org} $stock_{-1m}$ in the North Pacific (270 ± 52 Mg ha^{-1}) compared to the Gulf of Mexico (438 ± 76 Mg ha^{-1}), attributed to regional climates (lower C_{org} $stock_{-1m}$ arid and humid regions) and coastal geomorphology (limited habitat available for mangroves in the North Pacific).

The high variability in C_{org} $stock_{-1m}$ around the world is reflected in the wide range of values among countries (72–936 Mg ha^{-1}; Fig. 7; Atwood et al., 2017) and regions in Mexico (10–1952 Mg ha^{-1}; Herrera-Silveira et al., 2020), adds complexity to the general understanding of factors driving C_{org} accumulation and preservation in mangroves. The inclusion of data from diverse periods in databases (1985–2017, Atwood et al., 2017; 1996–2016, Herrera-Silveira et al., 2020) may introduce a potential limitation for stock comparison since this study (Fig. 4) and other publications employing dated sediment cores (e.g., Cuellar-Martinez et al., 2020; López-Mendoza et al., 2020) have demonstrated that C_{org} stocks vary over time. The present study proposes the establishment of C_{org} stock databases over comparable timeframes, such as 100 years (e.g., 1900–2000 or 1920–2020), employing reliable dating methods (e.g., ^{210}Pb). It also emphasizes the significance of standardizing measurement techniques and adopting best practices in sediment sampling and measurement to ensure consistency and comparability across assessments of C_{org} burial rates and stocks.

The CO_2 emission rates per ha resulting from sediment disturbance were higher in LTMCA03 than in other cores (Table 4). However, when accounting for the annual rate of mangrove loss, the PDE system has been releasing a larger volume of yearly CO_2 emissions (30.1 ± 0.4 Tg yr^{-1}) due to ongoing deforestation (Table 1). Although the overall range of potential CO_2 emissions in the study sites (501–883 Mg ha^{-1}) was lower than mean values estimated for mangroves worldwide (1415 Mg ha^{-1}; Howard et al., 2014), the conversion or degradation of these ecosystems could result in a higher amount of CO_2 emissions, considering potential disturbances extending beyond 1 m (Kauffman et al., 2020; Lovelock et al., 2017) and the exclusion of other possible greenhouse gas emissions such as CH_4 and N_2O (Macreadie et al., 2019). Mangrove protection and restoration efforts are crucial to mitigate these emissions and capitalize on this natural climate solution.

5.4. Temporal evolution of sources and its impact on burial rates and stocks

In all sediment cores, the increase by 5–41 % of the fluvial C_{org} contribution over the last century (Fig. 4) is associated with a rising flux of terrestrial elements (Al, Ca) and a shift in detrital sources shown by increasing values of the Al/Ti ratio (Fig. 5), indicating an increasing influence of river inputs across all the studied mangroves. This was consistent with the river discharge data (Fig. 5; data not available for the Quelite River) and previous studies that reported increasing discharges in the Usumacinta and Candelaria rivers since the 1950s, attributed to deforestation and land-use changes (Benítez et al., 2005; Fichez et al., 2017; Soto-Galera et al., 2010). Decreasing values of C:N ratios (except for 2021–2011 in specific cores; see Section 5.1) and variations in $\delta^{13}C$ and $\delta^{15}N$ values (Fig. 3) suggested progressive alterations in C_{org} inputs

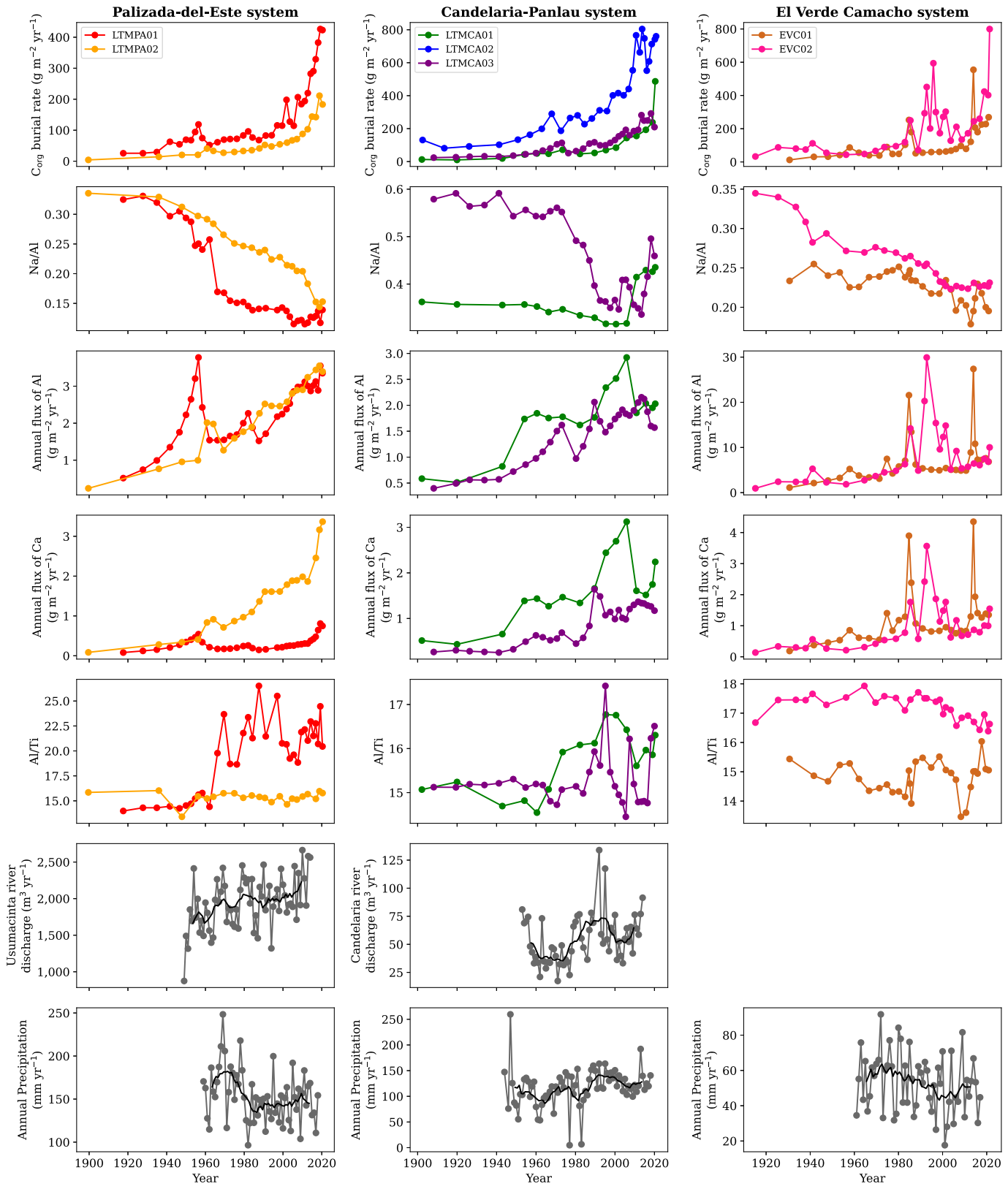

Fig. 5. Temporal variations in organic carbon and elemental accumulation in mangrove sediment cores from Términos Lagoon (southern Gulf of Mexico) and El Verde Camacho Lagoon (entrance of the Gulf of California). Annual river discharge and precipitation are shown in Table S1 in Supplementary Material.

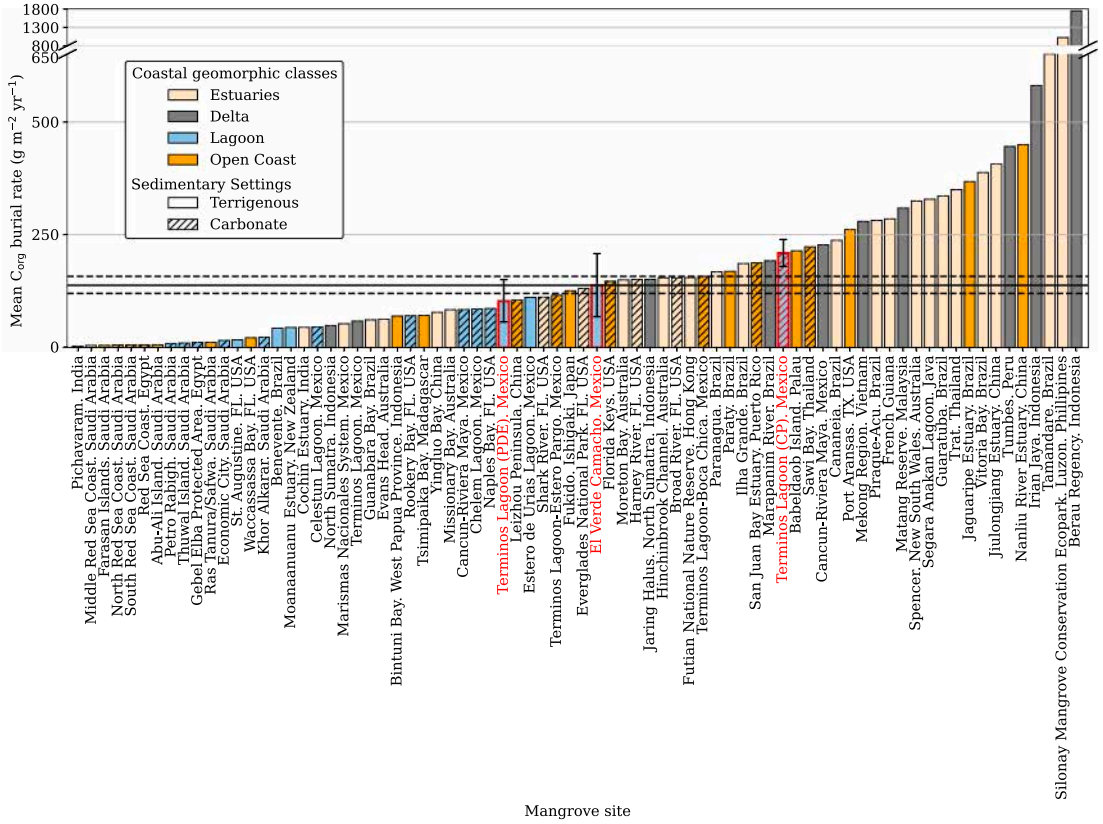

Fig. 6. Cross-comparison of organic carbon (C_{org}) burial rates in mangrove ecosystems worldwide. The sites from this study are represented with red bars. Horizontal black solid and dashed lines indicate the mean and 95 % confidence interval. PDE: Palizada-del-Este; CP: Candelaria-Panlau. The database was sourced from Breithaupt and Steinmuller (2022).

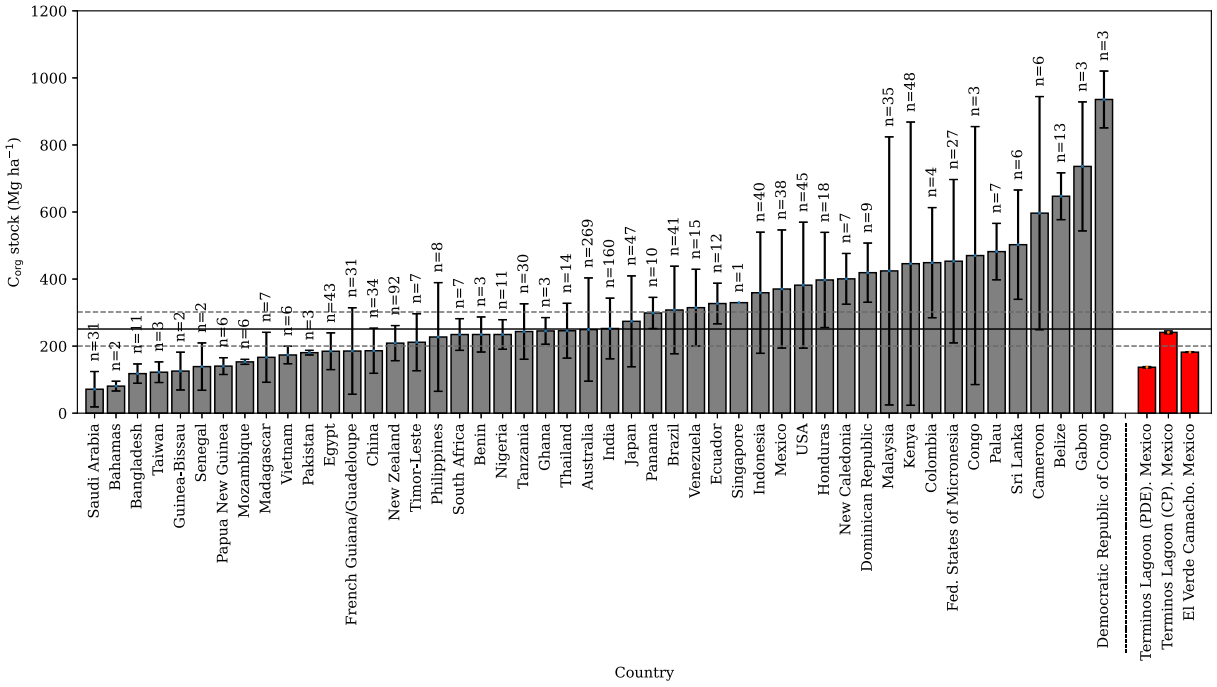

Fig. 7. Cross-comparison of organic carbon (C_{org}) stocks at 1 m depth in mangrove ecosystems worldwide. The sites from this study are represented with red bars. Horizontal black solid and dashed lines indicate the mean and 95 % confidence interval. PDE: Palizada-del-Este; CP: Candelaria-Panlau. The database was sourced from Atwood et al. (2017).

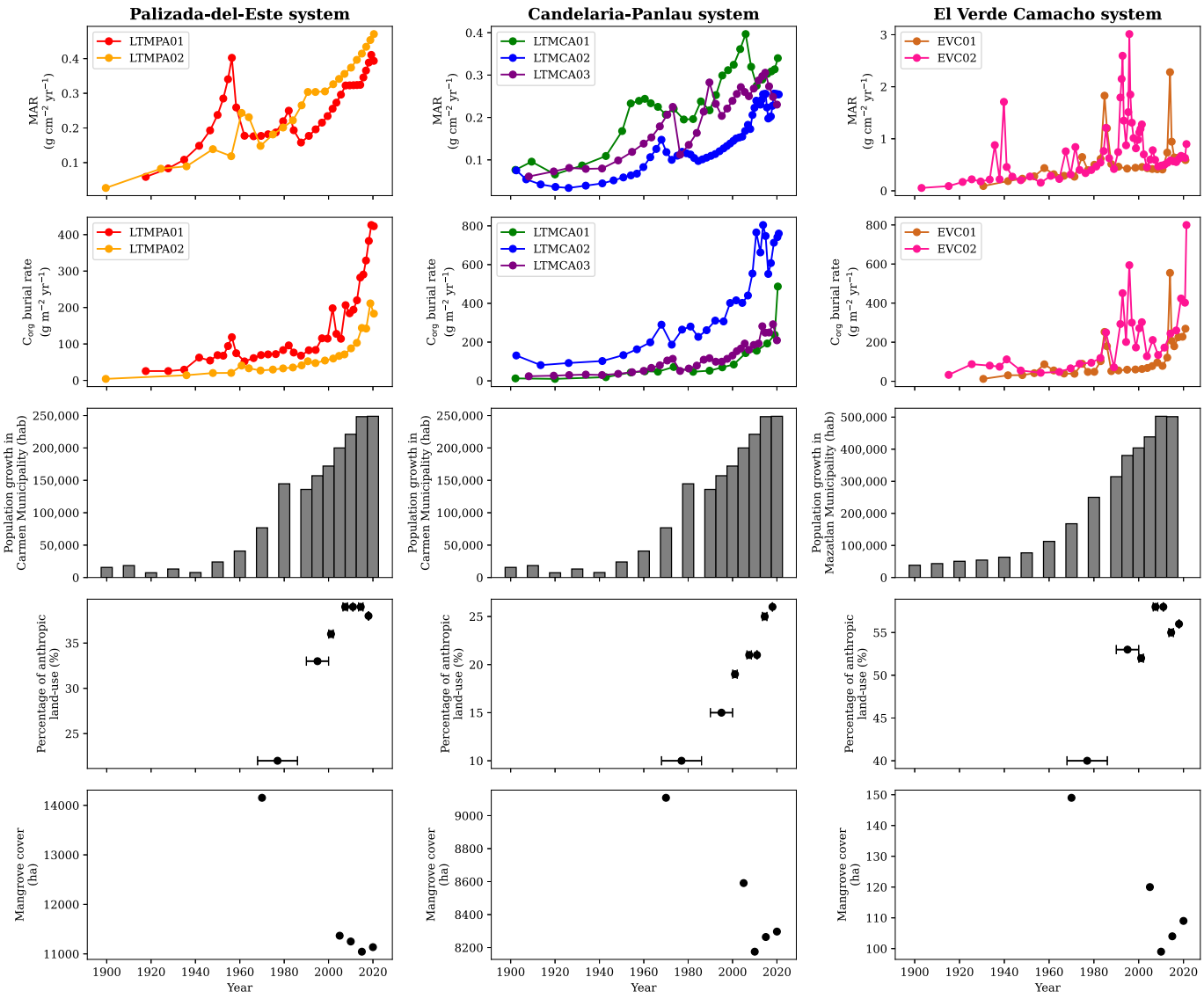

Fig. 8. Environmental factors affecting sediment and organic carbon (C_{org}) accumulation in Términos Lagoon (southern Gulf of Mexico) and El Verde Camacho Lagoon (entrance of the Gulf of California). MAR: Mass accumulation rate. References can be found in Table S2 in Supplementary Material.

or composition.

The rising trends in fluvial inputs and C_{org} burial rates coincided with the consistently increasing MAR trend and its acceleration after the 1950s (Fig. 8; Jupin et al., 2023). The determination coefficients of the regression between C_{org} burial rates and MAR indicated that MAR explained between 72 and 99 % of the increasing C_{org} burial rates in the study sites. The rise of MAR was attributed to a progressive change in sediment sources in the mangrove ecosystems. It was interpreted as an outcome of global factors (i.e., continental erosion and sea-level rise) influencing the temporal variability of sediment accumulation in the study sites (Jupin et al., 2023). Over the last century, the increase in continental erosion was driven by population growth and the consequential land-use changes within the river basins (Fig. 8). Within the study sites, it resulted in a progressive increase in C_{org} concentrations, burial rates, and stock$_{\text{-10yr}}$ (Figs. 3, 4, and 5) over the past century, with a majority of C_{org} stock$_{\text{-100yr}}$ (80–92 %) accumulated in the post-1950 period (Table 4), contradicting the research hypothesis. This phenomenon, documented in coastal areas worldwide (e.g., Ruiz-Fernández et al., 2009), has been previously associated with a consistent increase in C_{org} burial rates and stocks in some mangrove (e.g., Cuellar-Martinez et al., 2020) and seagrass meadow ecosystems (e.g., López-Mendoza et al., 2020; Ruiz-Fernández et al., 2020).

In the CP cores, the wider Bayesian credible intervals (5–95 %) during 1961–1981 than other time intervals were associated with a higher contribution of lagoon-derived C_{org} and a diminished contribution of fluvial C_{org} (Fig. 4). This was attributed to the occurrence of low precipitation conditions and reduced river discharge magnitudes (Fig. 5), potentially favoring marine intrusion during this period. In the subsequent decades (1980–2000) characterized by high river discharges and precipitation, there was a concurrent increase in the accumulation of Al and Ca and values of Al/Ti ratios observed in the cores LTMCA01 and LTMCA03 (Fig. 5), suggesting a substantial influx of terrigenous and carbonate sediment inputs, with a distinct mineralogical composition. The lowest Na/Al ratios were found during the same period, confirming a minor marine influence. In core EVC02, the observed increase in MAR and C_{org} burial rate (Fig. 8) from 1995 to 2005 coincided with the highest contributions of fluvial C_{org} in this core (Fig. 4), likely due to an intensified influence of the Quelite River.

Mangrove areas accumulated sediments in equilibrium with local sea-level rise in the TL and EV systems (Jupin et al., 2023). However, the decline in the contribution of marine or lagoon phytoplankton-derived C_{org} in the cores over the past century (Fig. 4), along with reducing

trends of the Na/Ti ratio (Fig. 5), suggested that the increasing dominance of fluvial C_{org} contribution has been outpacing the potential rise in C_{org} contributions associated with sea-level rise in the study sites. The decreasing contribution of phytoplankton-derived C_{org} was also evident in LTMCA02, characterized by a minor river influence, and was attributed to a progressive increase in the contribution of mangrove detritus during the study period (Fig. 4).

Besides LTMCA02, a growing mangrove contribution over the last century was also observed in several cores (LTMPA01, LTMCA01, and LTMCA03) and attributed to a combination of factors that could include i) a potential increase in mangrove aboveground productivity over time driven by rising nutrient inputs from the river (Morris et al., 2016), ii) a rise in surface elevation through biotic processes (root generation, microbial mat formation, and detritus accumulation) to compensate sea-level rise (McKee, 2011; Mckee et al., 2007), and iii) enhanced preservation of autochthonous C_{org}, facilitated by heightened sediment deposition and water flooding, effectively relocating C_{org} away from the surface and aerobic conditions (Burdige, 2007). These observations indicated that, although the mangrove cover was reduced in the study sites (Fig. 8), primarily resulting from deforestation for the development of intensive agriculture and urban settlements (Monjardín-Armenta et al., 2017; Soto-Galera et al., 2010), the remaining mangroves continue to play a crucial role as significant producers and sinks of in situ C_{org} in these sites, by adapting to the changing environmental conditions.

6. Conclusions

This research quantified source contributions and accumulation and storage capacity of sedimentary organic carbon over ~100 years by using geochemical data from seven ^{210}Pb-dated sediment cores collected in mangrove areas in the Términos Lagoon and El Verde Camacho Lagoon (Mexico). The distinction between cores with dominant fluvial contributions and those with dominant autochthonous contributions (mangrove detritus) was determined using the mixing model MixSIAR and attributed to the influence of local rivers on the origin, importation, and exportation of organic carbon within the sites. The highest burial rates and stocks were observed in mangrove areas with limited river influence and dominated by autochthonous inputs of organic carbon. The carbonate system Candelaria-Panlau, in Términos Lagoon, showed the highest accumulation and storage of sedimentary organic carbon, constituting the most effective sinks among sites. While general patterns based on coastal morphology and regional climate regimes have been identified globally, these patterns did not accurately apply to the local-scale variability observed in study sites. Burial rates and stocks generally increased over the past century, contradicting the initial hypothesis. This upward trend was mainly associated with the rising prevalence of organic material supplied by river systems, driven by continental erosion, and enhanced production and preservation of mangrove detritus. Despite the reported reduction in their cover within river basins, this study highlighted i) that mangroves continue to serve as influential producers and sinks of organic carbon and ii) the need for sustained efforts to improve databases, aiming to bolster their protection and facilitate restoration initiatives.

CRediT authorship contribution statement

J.L.J. Jupin: Conceptualization, Formal analysis, Investigation, Validation, Writing – original draft. **A.C. Ruiz-Fernández:** Writing – review & editing, Writing – original draft, Supervision, Resources, Project administration, Methodology, Investigation, Funding acquisition, Formal analysis, Data curation, Conceptualization. **A. Sifeddine:** Writing – review & editing, Funding acquisition, Conceptualization. **M. Mendez-Millan:** Writing – review & editing, Formal analysis, Data curation, Conceptualization. **J.A. Sanchez-Cabeza:** Conceptualization, Investigation, Methodology, Writing – review & editing. **L.H. Pérez-Bernal:** Data curation, Formal analysis, Methodology, Writing – review & editing. **J.G. Cardoso-Mohedano:** Formal analysis, Investigation, Methodology, Writing – review & editing. **M.A. Gómez-Ponce:** Formal analysis, Methodology, Writing – review & editing. **J.G. Flores-Trujillo:** Formal analysis, Investigation, Writing – review & editing.

Declaration of competing interest

The authors declare that they have no known competing financial interests or personal relationships that could have appeared to influence the work reported in this paper.

Data availability

Data will be made available on request.

Acknowledgments

This work was possible due to the support of the Universidad Nacional Autónoma de México (UNAM) through the project PAPIIT-DGAPA IN102821, and of the Institut de Recherche pour le Développement (IRD) through the international network DEXICOTROP and the Alysés platform facilities for geochemical and isotopic analyses. A Ph.D. fellowship provided by Consejo Nacional de Ciencia y Tecnología-Mexico (CONACYT, CVU 1102000) and the support of the Posgrado en Ciencias del Mar y Limnologia, UNAM, is acknowledged by Jupin J. L. J. Authors are grateful for the support received from M. Amador-Medina and J. C. Gonzalez-Palacios (Comisión Nacional de Áreas Naturales Protegidas del Santuario Plata El Verde Camacho), E. Ramírez-Tirado (El Recreo Community), J. A. Martinez-Trejo (sampling), L. F. Álvarez-Sánchez (data curation), I. Djouraev (data analysis), and C. Súarez-Gutiérrez (informatics).

Appendix A. Supplementary data

Supplementary data to this article can be found online at https://doi.org/10.1016/j.scitotenv.2024.173440.

References

Adame, M.F., Fry, B., 2016. Source and stability of soil carbon in mangrove and freshwater wetlands of the Mexican Pacific coast. Wetl. Ecol. Manag. 24, 129–137. https://doi.org/10.1007/s11273-015-9475-6.

Allais, L., Thibodeau, B., Khan, N.S., Crowe, S.A., Cannicci, S., Not, C., 2024. Salinity, mineralogy, porosity, and hydrodynamics as drivers of carbon burial in urban mangroves from a megacity. Sci. Total Environ. 912, 168955 https://doi.org/10.1016/j.scitotenv.2023.168955.

Alongi, D.M., 2014. Carbon cycling and storage in mangrove forests. Ann. Rev. Mar. Sci. 6, 195–219. https://doi.org/10.1146/annurev-marine-010213-135020.

Atwood, T.B., Connolly, R.M., Almahasheer, H., Carnell, P.E., Duarte, C.M., Lewis, C.J.E., Irigoien, X., Kelleway, J.J., Lavery, P.S., Macreadie, P.I., Serrano, O., Sanders, C.J., Santos, I.R., Steven, A.D.L., Lovelock, C.E., 2017. Global patterns in mangrove soil carbon stocks and losses. Nat. Clim. Chang. 7, 523–528. https://doi.org/10.1038/nclimate3326.

Bach, L., Calderon, R., Cepeda, M.F., Oczkowski, A., Olsen, S.B., Robadue, D., 2005. Resumen del Perfil de Primer Nivel del Sitio Laguna de Términos y su Cuenca, México, Coastal Resources Center. University of Rhode Island. Coastal Resources Center, University of Rhode Island, Narragansett.

Benítez, J.A., Sanvicente Sánchez, H., Lafragua Contreras, J., Zamora Crescencio, P., Morales Manilla, L.M., Mas Caussel, J.F., García Gil, G., Couturier, S.A., Zetina Tapia, R., Calan Yam, R.A., Amabilis Sánchez, L., Acuña, C., Mejenes, M., 2005. Sistemas de información geográfica de la cuenca del río Candelaria: reconstrucción histórica de los cambios de cobertura forestal y su efecto sobre la hidrología y calidad del agua-marco teórico y resultados iniciales. In: Edith, F., Kauffer, M. (Eds.), El Agua En La Frontera México-Guatemala-Belice. Ecosur/tnc/unach, Tuxtla Gutiérrez, Chiapas, pp. 19–32.

Blaauw, M., Christen, J.A., Aquino-López, M.A., Esquivel-Vazquez, J., Gonzalez, O.M., Belding, T., Theiler, J., Gough, B., Karney, C., 2021. Bayesian age-depth modelling of cores dated by Pb-210. https://cran.r-project.org/web/packages/rplum/rplum.pdf.

Blankespoor, B., Dasgupta, S., Lange, G.-M., 2017. Mangroves as a protection from storm surges in a changing climate. Ambio 46, 478–491. https://doi.org/10.1007/s13280-016-0838-x.

Bouillon, S., Dahdouh-Guebas, F., Rao, A.V.V.S., Koedam, N., Dehairs, F., 2003. Sources of organic carbon in mangrove sediments: variability and possible ecological

implications. Hydrobiologia 495, 33–39. https://doi.org/10.1023/A:1025411506526.
Bouillon, S., Connolly, R.M., Lee, S.Y., 2008. Organic matter exchange and cycling in mangrove ecosystems: recent insights from stable isotope studies. J. Sea Res. 59, 44–58. https://doi.org/10.1016/j.seares.2007.05.001.
Breithaupt, J.L., Steinmuller, H.E., 2022. Refining the global estimate of mangrove carbon burial rates using sedimentary and geomorphic settings. Geophys. Res. Lett. 49 https://doi.org/10.1029/2022GL100177.
Breithaupt, J.L., Smoak, J.M., Smith, T.J., Sanders, C.J., Hoare, A., 2012. Organic carbon burial rates in mangrove sediments: strengthening the global budget. Global Biogeochem. Cycles 26, 1–11. https://doi.org/10.1029/2012GB004375.
Brett, M.T., 2014. Resource polygon geometry predicts Bayesian stable isotope mixing model bias. Mar. Ecol. Prog. Ser. Inter-Research 514, 1–12. https://doi.org/10.3354/meps11017.
Briseño-Dueñas, R., 2003. Ficha Informativa de los Humedales de Ramsar (FIR). "Playa Tortuguera El Verde Camacho" [WWW Document]. URL. https://rsis.ramsar.org/RISapp/files/RISrep/MX1349RIS.pdf.
Burdige, D.J., 2007. Linking sediment organic geochemistry and sediment diagenesis. In: Geochemistry of Marine Sediments. Princeton University Press, Princeton, pp. 237–270. https://doi.org/10.1515/9780691216096-013.
Carter, S., Fisher, A., Garcia, R., Gibson, B., Lancaster, S., Marshall, J., Whiteside, I., 2015. Atomic spectrometry update. Review of advances in the analysis of metals, chemicals and functional materials. J. Anal. At. Spectrom 30, 2249–2294. https://doi.org/10.1039/C5JA90045J.
Cerón-Bretón, J.G., Cerón-Bretón, R.M., Rangel-marrón, M.M., Muriel-García, M., Cordova-Quiroz, A.V., Estrella-Cahuich, A., 2011. Determination of carbon sequestration rate in soil of a mangrove forest in Campeche, Mexico. WSEAS Trans. Environ. Dev. 7, 54–64.
Cifuentes, L.A., Coffin, R.B., Solorzano, L., Cardenas, W., Espinoza, J., Twilley, R.R., 1996. Isotopic and elemental variations of carbon and nitrogen in a mangrove estuary. Estuar. Coast. Shelf Sci. 43, 781–800. https://doi.org/10.1006/ecss.1996.0103.
CONABIO, 2013. Distribución de los manglares en México en 1970-1981, escala: 1: 50000. edición: 1. Proyecto: GQ004, Los manglares de México: Estado actual y establecimiento de un programa de monitoreo a largo [WWW Document]. Comisión Nacional para el Conocimiento y Uso de la Biodiversidad. URL. http://geoportal.conabio.gob.mx/metadatos/doc/html/mexman70gw.html (accessed 1.2.23).
CONABIO, 2021. Distribución de los manglares en México en 2020, escala: 1:50000. edición: 1. Sistema de Monitoreo de los Manglares de México (SMMM). [WWW Document]. Comisión Nacional para el Conocimiento y Uso de la Biodiversidad. URL. http://geoportal.conabio.gob.mx/metadatos/doc/html/mx_man20gw.html (accessed 1.2.23).
CONAGUA, 2015. Determinación de la Disponibilidad de Agua en el acuífero Río Quelite, estado de Sinaloa. Comisión Nacional del Agua CONAGUA.
Contreras-Ruiz-Esparza, A., Douillet, P., Zavala-Hidalgo, J., 2014. Tidal dynamics of the Terminos Lagoon, Mexico: observations and 3D numerical modelling. Ocean Dyn. 64, 1349–1371. https://doi.org/10.1007/s10236-014-0752-3.
Cotler-Ávalos, H., 2010. Las cuencas hidrograficas de México. Diagnostico y Priorizacion, Secretaría de Medio Ambiente y Recursos Naturales. Instituto Nacional de Ecología. Pluralia Ediciones e Impresiones, México, D.F.
Croudace, I.W., Rothwell, R.G., 2015. Micro-XRF Studies of Sediment Cores, Developments in Paleoenvironmental Research. Springer, Netherlands, Dordrecht. https://doi.org/10.1007/978-94-017-9849-5.
Cuellar-Martinez, T., Ruiz-Fernández, A.C., Sanchez-Cabeza, J.A., Pérez-Bernal, L.H., Sandoval-Gil, J., 2019. Relevance of carbon burial and storage in two contrasting blue carbon ecosystems of a north-east Pacific coastal lagoon. Sci. Total Environ. 675, 581–593. https://doi.org/10.1016/j.scitotenv.2019.03.388.
Cuellar-Martinez, T., Ruiz-Fernández, A.C., Sanchez-Cabeza, J.A., Pérez-Bernal, L., López-Mendoza, P.G., Carnero-Bravo, V., Agraz-Hernández, C.M., van Tussenbroek, B.I., Sandoval-Gil, J., Cardoso-Mohedano, J.G., Vázquez-Molina, Y., Aldana-Gutiérrez, G., 2020. Temporal records of organic carbon stocks and burial rates in Mexican blue carbon coastal ecosystems throughout the Anthropocene. Glob. Planet Change 192, 103215. https://doi.org/10.1016/j.gloplacha.2020.103215.
Díaz-Asencio, M., Sanchez-Cabeza, J.A., Ruiz-Fernández, A.C., Corcho-Alvarado, J.A., Pérez-Bernal, L.H., 2020. Calibration and use of well-type germanium detectors for low-level gamma-ray spectrometry of sediments using a semi-empirical method. J. Environ. Radioact. 225 https://doi.org/10.1016/j.jenvrad.2020.106385.
Douglas, P.M.J., Stratigopoulos, E., Park, S., Keenan, B., 2022. Spatial differentiation of sediment organic matter isotopic composition and inferred sources in a temperate forest lake catchment. Chem. Geol. 603 https://doi.org/10.1016/j.chemgeo.2022.120887.
FAO, 2007. The World's Mangroves 1980–2005: A Thematic Study Prepared in the Framework of the Global Forest Resources Assessment 2005. FAO Forestry Paper, Rome.
Fichez, R., Archundia, D., Grenz, C., Douillet, P., Gutiérrez-Mendieta, F., Origel-Moreno, M., Denis, L., Contreras-Ruiz-Esparza, A., Zavala-Hidalgo, J., 2017. Global climate change and local watershed management as potential drivers of salinity variation in a tropical coastal lagoon (Laguna de Terminos, Mexico). Aquat. Sci. 79, 219–230. https://doi.org/10.1007/s00027-016-0492-1.
Flores-Verdugo, F.J., Day, J.W., Briseño-Dueñas, R., 1987. Structure, litter fall, decomposition, and detritus dynamics of mangroves in a Mexican coastal lagoon with an ephemeral inlet. Mar. Ecol. Prog. Ser. 35, 83–90.
Flores-Verdugo, F.J., Briseño-Dueñas, R., González-Farías, F., Calvario-Martínez, O., 1995. Balance de carbono en un ecosistema lagunar estuarino de boca efímera de la costa noroccidental de México (Estero El Verde, Sinaloa). In: Temas de oceanografía biológica en México. Universidad Autónoma de Baja California, Ensenada, 8.C., México. II.
García, E., 1973. Modificaciones al sistema de clasificación climática de Köppen: para adaptarlo a las condiciones de la república mexicana, 6th ed. Universidad Nacional Autónoma de México, México, D. F.
Goldberg, L., Lagomasino, D., Thomas, N., Fatoyinbo, T., 2020. Global declines in human-driven mangrove loss. Glob. Chang. Biol. 26, 5844–5855. https://doi.org/10.1111/gcb.15275.
Gonneea, M.E., Paytan, A., Herrera-Silveira, J.A., 2004. Tracing organic matter sources and carbon burial in mangrove sediments over the past 160 years. Estuar. Coast. Shelf Sci. 61, 211–227. https://doi.org/10.1016/j.ecss.2004.04.015.
González-Farías, F., Mee, L.D., 1988. Effect of mangrove humic-like substances on biodegradation rate of detritus. J. Exp. Mar. Biol. Ecol. 119, 1–13. https://doi.org/10.1016/0022-0981(88)90148-7.
Guerra-Santos, J.J., Cerón-Bretón, R.M., Cerón-Bretón, J.G., Damián-Hernández, D.L., Sánchez-Junco, R.C., Guevara-Carrió, E.C., 2014. Estimation of the carbon pool in soil and above-ground biomass within mangrove forests in Southeast Mexico using allometric equations. J. For. Res. (Harbin) 25, 129–134. https://doi.org/10.1007/s11676-014-0437-2.
Hamilton, S.E., Casey, D., 2016. Creation of a high spatio-temporal resolution global database of continuous mangrove forest cover for the 21st century (CGMFC-21). Glob. Ecol. Biogeogr. 25, 729–738. https://doi.org/10.1111/geb.12449.
Hamilton, S.E., Friess, D.A., 2018. Global carbon stocks and potential emissions due to mangrove deforestation from 2000 to 2012. Nat. Clim. Chang. 8, 240–244. https://doi.org/10.1038/s41558-018-0090-4.
Herrera-Silveira, J.A., Camacho-Rico, A., Pech, E., Pech, M., Ramírez-Ramírez, J., Teutli-Hernández, C., 2016. Carbon dynamics (stocks and fluxes) in mangroves of Mexico. Terra Latinoamericana 34–I, 61–72.
Herrera-Silveira, J.A., Pech-Cardenas, M.A., Morales-Ojeda, S.M., Cinco-Castro, S., Camacho-Rico, A., Caamal-Sosa, J.P., Mendoza-Martinez, J.E., Pech-Poot, E.Y., Montero, J., Teutli-Hernández, C., 2020. Blue carbon of Mexico, carbon stocks and fluxes: a systematic review. PeerJ 8, e8790. https://doi.org/10.7717/peerj.8790.
Coastal blue carbon: methods for assessing carbon stocks and emissions factors in mangroves, tidal salt marshes, and seagrasses. In: Howard, J., Hoyt, S., Isensee, K., Telszewski, M., Pidgeon, E. (Eds.), 2014. Conservational International, Intergovernmental Oceanographic Commission of UNESCO. International Union for Conservation of Nature, Arlington, Virginia, USA.
Jennerjahn, T.C., 2020. Relevance and magnitude of "blue carbon" storage in mangrove sediments: carbon accumulation rates vs. stocks, sources vs. sinks. Estuar. Coast. Shelf Sci. 247, 107027 https://doi.org/10.1016/j.ecss.2020.107027.
Jupin, J.L.J., Ruiz-Fernández, A.C., Sifeddine, A., Sanchez-Cabeza, J.A., Pérez-Bernal, L. H., Cardoso-Mohedano, J.G., Gómez-Ponce, M.A., Flores-Trujillo, J.G., 2023. Anthropogenic drivers of increasing sediment accumulation in contrasting Mexican mangrove ecosystems. Catena (Amst) 226, 107037. https://doi.org/10.1016/j.catena.2023.107037.
Kauffman, J.B., Heider, C., Norfolk, J., Payton, F., 2014. Carbon stocks of intact mangroves and carbon emissions arising from their conversion in the Dominican Republic. Ecol. Appl. 24, 518–527. https://doi.org/10.1890/13-0640.1.
Kauffman, J.B., Adame, M.F., Arifanti, V.B., Schile-Beers, L.M., Bernardino, A.F., Bhomia, R.K., Donato, D.C., Feller, I.C., Ferreira, T.O., Jesus Garcia, M. del C., MacKenzie, R.A., Megonigal, J.P., Murdiyarso, D., Simpson, L., Hernández Trejo, H., 2020. Total ecosystem carbon stocks of mangroves across broad global environmental and physical gradients. Ecological monographs 90. https://doi.org/10.1002/ecm.1405.
Kusumaningtyas, M.A., Hutahaean, A.A., Fischer, H.W., Pérez-Mayo, M., Ransby, D., Jennerjahn, T.C., 2019. Variability in the organic carbon stocks, sources, and accumulation rates of Indonesian mangrove ecosystems. Estuar. Coast. Shelf Sci. 218, 310–323. https://doi.org/10.1016/j.ecss.2018.12.007.
Lallier-Vergès, E., Perrussel, B.P., Disnar, J.R., Baltzer, F., 1998. Relationships between environmental conditions and the diagenetic evolution of organic matter derived from higher plants in a modern mangrove swamp system (Guadeloupe, French West Indies). Org. Geochem. 29, 1663–1686. https://doi.org/10.1016/S0146-6380(98)00179-X.
Lavery, P., Lafratta, A., Serrano, O., Masque, P., Jones, A., Fernandes, M., Gaylard, S., Gillanders, B., 2019. Coastal carbon opportunities: carbon storage and accumulation rates at three case study sites. In: Technical Report Series No. 19/21 (Adelaide).
López-Mendoza, P.G., Ruiz-Fernández, A.C., Sanchez-Cabeza, J.A., van Tussenbroek, B.I., Cuellar-Martinez, T., Pérez-Bernal, L.H., 2020. Temporal trends of organic carbon accumulation in seagrass meadows from the northern Mexican Caribbean. Catena (Amst.) 194, 104645. https://doi.org/10.1016/j.catena.2020.104645.
Lovelock, C.E., Fourqurean, J.W., Morris, J.T., 2017. Modeled CO2 emissions from coastal wetland transitions to other land uses: tidal marshes, mangrove forests, and seagrass beds. Front. Mar. Sci. 4, 1–11. https://doi.org/10.3389/fmars.2017.00143.
Macreadie, P.I., Anton, A., Raven, J.A., Beaumont, N.J., Connolly, R.M., Friess, D.A., Kelleway, J.J., Kennedy, H., Kuwae, T., Lavery, P.S., Lovelock, C.E., Smale, D.A., Apostolaki, E.T., Atwood, T.B., Baldock, J.A., Bianchi, T.S., Chmura, G.L., Eyre, B.D., Fourqurean, J.W., Hall-Spencer, J.M., Huxham, M., Hendriks, I.E., Krause-Jensen, D., Laffoley, D., Luisetti, T., Marbà, N., Masque, P., McGlathery, K.J., Megonigal, J.P., Murdiyarso, D., Russell, B.D., Santos, I.R., Serrano, O., Silliman, B. R., Watanabe, K., Duarte, C.M., 2019. The future of blue carbon science. Nat. Commun. 10, 1–13. https://doi.org/10.1038/s41467-019-11693-w.
Marchand, C., Disnar, J.R., Lallier-Vergès, E., Lottier, N., Lallier-Vergès, E., Lottier, N., 2005. Early diagenesis of carbohydrates and lignin in mangrove sediments subject to variable redox conditions (French Guiana). Geochim. Cosmochim. Acta 69, 131–142. https://doi.org/10.1016/j.gca.2004.06.016.

McKee, K.L., 2011. Biophysical controls on accretion and elevation change in Caribbean mangrove ecosystems. Estuar. Coast. Shelf Sci. 91, 475–483. https://doi.org/10.1016/j.ecss.2010.05.001.

Mckee, K.L., Cahoon, D.R., Feller, I.C., 2007. Caribbean mangroves adjust to rising sea level through biotic controls on change in soil elevation. Glob. Ecol. Biogeogr. 16, 545–556. https://doi.org/10.1111/j.1466-8238.2007.00317.x.

Medina-Contreras, D., Sánchez, A., Arenas, F., 2023. Macroinvertebrates food web and trophic relations of a peri urban mangrove system in a semi-arid region, Gulf of California, México. J. Mar. Syst. 240 https://doi.org/10.1016/j.jmarsys.2023.103864.

Medina-Gómez, I., Villalobos-Zapata, G.J., Herrera-Silveira, J.A., 2015. Spatial and temporal hydrological variations in the inner estuaries of a large coastal lagoon of the Southern Gulf of Mexico. J. Coast. Res. 316, 1429–1438. https://doi.org/10.2112/jcoastres-d-13-00226.1.

Menges, J., Hovius, N., Andermann, C., Lupker, M., Haghipour, N., Märki, L., Sachse, D., 2020. Variations in organic carbon sourcing along a trans-Himalayan river determined by a Bayesian mixing approach. Geochim. Cosmochim. Acta 286, 159–176. https://doi.org/10.1016/j.gca.2020.07.003.

Meyers, P.A., 1997. Organic geochemical proxies of paleoceanographic, paleolimnologic, and paleoclimatic processes. Org. Geochem. 27, 213–250. https://doi.org/10.1016/S0146-6380(97)00049-1.

Monjardín-Armenta, S.A., Pacheco-Angulo, C.E., Plata-Rocha, W., Corrales-Barraza, G., 2017. La deforestación and sus factores causales en el estado de Sinaloa, México. Madera Bosques 23, 7–22. https://doi.org/10.21829/myb.2017.2311482.

Moore, J.W., Semmens, B.X., 2008. Incorporating uncertainty and prior information into stable isotope mixing models. Ecol. Lett. 11, 470–480. https://doi.org/10.1111/j.1461-0248.2008.01163.x.

Morris, J.T., Barber, D.C., Callaway, J.C., Chambers, R., Hagen, S.C., Hopkinson, C.S., Johnson, B.J., Megonigal, P., Neubauer, S.C., Troxler, T., Wigand, C., 2016. Contributions of organic and inorganic matter to sediment volume and accretion in tidal wetlands at steady state. Earths Futur. 4, 110–121. https://doi.org/10.1002/2015EF000334.

Murdiyarso, D., Purbopuspito, J., Kauffman, J.B., Warren, M.W., Sasmito, S.D., Donato, D.C., Manuri, S., Krisnawati, H., Taberima, S., Kurnianto, S., 2015. The potential of Indonesian mangrove forests for global climate change mitigation. Nat. Clim. Chang. 5, 1089–1092. https://doi.org/10.1038/nclimate2734.

Ochoa, E.P., 2003. Ficha Informativa de los Humedales de Ramsar (FIR), pp. 1–17.

Ortiz-Pérez, M.A., de la Lanza-Espino, G., 2006. Diferenciación del espacio costero de México: un inventario regional. Geografía para el Siglo XXI. Universidad Nacional Autónoma de México, Instituto de Geografía, CDMX.

Parnell, A.C., Inger, R., Bearhop, S., Jackson, A.L., 2010. Source partitioning using stable isotopes: coping with too much variation. PloS One 5. https://doi.org/10.1371/journal.pone.0009672.

Parnell, A.C., Phillips, D.L., Bearhop, S., Semmens, B.X., Ward, E.J., Moore, J.W., Jackson, A.L., Grey, J., Kelly, D.J., Inger, R., 2013. Bayesian stable isotope mixing models. Environmetrics 24, 387–399. https://doi.org/10.1002/env.2221.

Pendleton, L., Donato, D.C., Murray, B.C., Crooks, S., Jenkins, W.A., Sifleet, S., Craft, C., Fourqurean, J.W., Kauffman, J.B., Marbà, N., Megonigal, P., Pidgeon, E., Herr, D., Gordon, D., Baldera, A., 2012. Estimating global "blue carbon" emissions from conversion and degradation of vegetated coastal ecosystems. PloS One 7, e43542. https://doi.org/10.1371/journal.pone.0043542.

Pérez, A., Libardoni, B.G., Sanders, C.J., 2018. Factors influencing organic carbon accumulation in mangrove ecosystems. Biol. Lett. 14, 20180237. https://doi.org/10.1098/rsbl.2018.0237.

Primavera, Jurgenne H., Friess, D.A., Van Lavieren, H., Lee, S.Y., 2019a. The mangrove ecosystem. In: Press, Academic (Ed.), World Seas: An Environmental Evaluation. Elsevier, pp. 1–34. https://doi.org/10.1016/B978-0-12-805052-1.00001-2.

Primavera, J.H., Friess, D.A., Van Lavieren, H., Lee, S.Y., 2019b. The mangrove ecosystem. In: World Seas: An Environmental Evaluation Volume III: Ecological Issues and Environmental Impacts, 2nd ed. Elsevier Ltd. https://doi.org/10.1016/B978-0-12-805052-1.00001-2 666p.

Ramos-Miranda, J., Villalobos-Zapata, G.J., 2015. Aspectos socioambientales de la región de la laguna de Términos. Universidad Autónoma de Campeche, Campeche.

Rendón-Von Osten, J., Memije, M.G., Ortiz, A., Soares, A.M.V.M., Guilhermino, L., 2006. An integrated approach to assess water quality and environmental contamination in the fluvial-lagoon system of the Palizada River, Mexico. Environ. Toxicol. Chem. 25, 3024–3034. https://doi.org/10.1897/05-491R.1.

Rosentreter, J.A., Maher, D.T., Erler, D.V., Murray, R.H., Eyre, B.D., 2018. Seasonal and temporal CO2 dynamics in three tropical mangrove creeks – a revision of global mangrove CO2 emissions. Geochim. Cosmochim. Acta 222, 729–745. https://doi.org/10.1016/j.gca.2017.11.026.

Ruiz-Fernández, A.C., Hillaire-Marcel, C., de Vernal, A., Machain-Castillo, M.L., Vásquez, L., Ghaleb, B., Aspiazu-Fabián, J.A., Páez-Osuna, F., 2009. Changes of coastal sedimentation in the Gulf of Tehuantepec, South Pacific Mexico, over the last 100 years from short-lived radionuclide measurements. Estuar. Coast. Shelf Sci. 82, 525–536. https://doi.org/10.1016/j.ecss.2009.02.019.

Ruiz-Fernández, A.C., Agraz-Hernández, C.M., Sanchez-Cabeza, J.A., Díaz-Asencio, M., Pérez-Bernal, L.H., Chan Keb, C.A., López-Mendoza, P.G., Blanco y Correa, J.M., Ontiveros-Cuadras, J.F., Osti Saenz, J., Reyes Castellanos, J.E., 2018a. Sediment geochemistry, accumulation rates and forest structure in a large tropical mangrove ecosystem. Wetlands 38, 307–325. https://doi.org/10.1007/s13157-017-0969-2.

Ruiz-Fernández, A.C., Carnero-Bravo, V., Sánchez-Cabeza, J.A., Pérez-Bernal, L.H., Amaya-Monterrosa, O.A., Bojórquez-Sánchez, S., López-Mendoza, P.G., Cardoso-Mohedano, J.G., Dunbar, R.B., Mucciarone, D.A., Marmolejo-Rodríguez, A.J., 2018b. Carbon burial and storage in tropical salt marshes under the influence of sea level rise. Sci. Total Environ. 630, 1628–1640. https://doi.org/10.1016/j.scitotenv.2018.02.246.

Ruiz-Fernández, A.C., Sanchez-Cabeza, J.A., Cuéllar-Martínez, T., Pérez-Bernal, L.H., Carnero-Bravo, V., Ávila, E., Cardoso-mohedano, J.G., Sanchez-Cabeza, J.A., Cuéllar-Martínez, T., Pérez-Bernal, L.H., Carnero-Bravo, V., Ávila, E., Cardoso-mohedano, J.G., 2020. Increasing salinization and organic carbon burial rates in seagrass meadows from an anthropogenically-modified coastal lagoon in southern Gulf of Mexico. Estuar. Coast. Shelf Sci. 242, 106843 https://doi.org/10.1016/j.ecss.2020.106843.

Sanchez-Cabeza, J.A., Ruiz-Fernández, A.C., 2012. 210Pb sediment radiochronology: an integrated formulation and classification of dating models. Geochim. Cosmochim. Acta 82, 183–200. https://doi.org/10.1016/j.gca.2010.12.024.

Sanchez-Cabeza, J.A., Ruiz-Fernández, A.C., Ontiveros-Cuadras, J.F., Pérez Bernal, L.H., Olid, C., 2014. Monte Carlo uncertainty calculation of 210Pb chronologies and accumulation rates of sediments and peat bogs. Quat. Geochronol. 23, 80–93. https://doi.org/10.1016/j.quageo.2014.06.002.

Sasmito, S.D., Kuzyakov, Y., Lubis, A.A., Murdiyarso, D., Hutley, L.B., Bachri, S., Friess, D.A., Martius, C., Borchard, N., 2020. Organic carbon burial and sources in soils of coastal mudflat and mangrove ecosystems. Catena (Amst.) 187, 104414. https://doi.org/10.1016/j.catena.2019.104414.

Sepúlveda-Lozada, A., Mendoza-Carranza, M., Wolff, M., Saint-Paul, U., Ponce-Mendoza, A., 2015. Differences in food web structure of mangroves and freshwater marshes: evidence from stable isotope studies in the southern Gulf of Mexico. Wetl. Ecol. Manag. 23, 293–314. https://doi.org/10.1007/s11273-014-9382-2.

Sepúlveda-Lozada, A., Saint-Paul, U., Mendoza-Carranza, M., Wolff, M., Yáñez-Arancibia, A., 2017. Flood pulse induced changes in isotopic niche and resource utilization of consumers in a Mexican floodplain system. Aquat. Sci. 79, 597–616. https://doi.org/10.1007/s00027-017-0520-9.

Sidik, F., Friess, D.A., 2021. Dynamic Sedimentary Environments of Mangrove Coasts. Elsevier. https://doi.org/10.1016/C2018-0-00130-9.

Smoak, J.M., Breithaupt, J.L., Smith, T.J., Sanders, C.J., 2013. Sediment accretion and organic carbon burial relative to sea-level rise and storm events in two mangrove forests in Everglades National Park. Catena (Amst.) 104, 58–66. https://doi.org/10.1016/j.catena.2012.10.009.

Soria-Barreto, M., Montaña, C.G., Winemiller, K.O., Castillo, M.M., Rodiles-Hernández, R., 2021. Seasonal variation in basal resources supporting fish biomass in longitudinal zones of the Usumacinta River Basin, southern Mexico. Mar. Freshw. Res. 72, 353–364. https://doi.org/10.1071/MF19341.

Soto-Galera, E., Piera, J., López, P., 2010. Spatial and temporal land cover changes in Terminos Lagoon Reserve, Mexico. Rev. Biol. Trop. 58, 565–575. https://doi.org/10.15517/rbt.v58i2.5229.

Stock, B., Semmens, B., 2016a. Unifying error structures in commonly used biotracer mixing models. Ecology 97, 2562–2569. https://doi.org/10.1002/ecy.1517.

Stock, B., Semmens, B., 2016b. MixSIAR GUI User Manual v3.1 (Version 3.1).

Stock, B.C., Jackson, A.L., Ward, E.J., Parnell, A.C., Phillips, D.L., Semmens, B.X., 2018. Analyzing mixing systems using a new generation of Bayesian tracer mixing models. PeerJ 6, e5096. https://doi.org/10.7717/peerj.5096.

UN, 2015. on Climate Change (21st Session, Paris). United Nations, p. 25. https://unfccc.int/sites/default/files/english_paris_agreement.pdf.

Valiela, I., Bowen, J.L., York, J.K., 2001. Mangrove forests: one of the world's threatened major tropical environments. Bioscience 51, 807–815. https://doi.org/10.1641/0006-3568(2001)051[0807:MFOOTW]2.0.CO;2.

Woodroffe, C.D., Rogers, K., McKee, K.L., Lovelock, C.E., Mendelssohn, I.A., Saintilan, N., 2016. Mangrove sedimentation and response to relative sea-level rise. Ann. Rev. Mar. Sci. 8, 243–266. https://doi.org/10.1146/annurev-marine-122414-034025.

Yáñez-Arancibia, A., Day, J.W., 1982. Ecological characterization of Terminos Lagoon, a tropical lagoon-estuarine system in the southern Gulf of Mexico. Oceanol. Acta 5, 431–440.